

Submit a Manuscript: <https://www.f6publishing.com>*World J Hepatol* 2022 May 27; 14(5): 923-943DOI: [10.4254/wjh.v14.i5.923](https://doi.org/10.4254/wjh.v14.i5.923)

ISSN 1948-5182 (online)

MINIREVIEWS

## Benign focal liver lesions: The role of magnetic resonance imaging

Marco Gatti, Cesare Maino, Davide Tore, Andrea Carisio, Fatemeh Darvizeh, Eleonora Tricarico, Riccardo Inchigolo, Davide Ippolito, Riccardo Faletti

**Specialty type:** Gastroenterology and hepatology

**Provenance and peer review:**  
Invited article; Externally peer reviewed

**Peer-review model:** Single blind

**Peer-review report's scientific quality classification**

Grade A (Excellent): 0

Grade B (Very good): B

Grade C (Good): 0

Grade D (Fair): 0

Grade E (Poor): 0

**P-Reviewer:** Gamarra LF, Brazil

**Received:** April 18, 2021

**Peer-review started:** April 18, 2021

**First decision:** July 27, 2021

**Revised:** August 7, 2021

**Accepted:** April 9, 2022

**Article in press:** April 9, 2022

**Published online:** May 27, 2022



**Marco Gatti, Davide Tore, Andrea Carisio, Riccardo Faletti**, Department of Surgical Sciences, University of Turin, Turin 10126, Italy

**Cesare Maino, Davide Ippolito**, Department of Diagnostic Radiology, Ospedale San Gerardo, Monza 20900, Italy

**Fatemeh Darvizeh**, School of Medicine, Vita-Salute San Raffaele University, Milan 20121, Japan

**Eleonora Tricarico**, Department of Radiology, “F. Perinei” Hospital, Altamura 70022, Italy

**Riccardo Inchigolo**, Interventional Radiology Unit, “F. Miulli” Regional General Hospital, Acquaviva delle Fonti 70021, Italy

**Davide Ippolito**, Department of Diagnostic Radiology, School of Medicine, University of Milano-Bicocca, Monza 20900, Italy

**Corresponding author:** Marco Gatti, MD, Research Fellow, Department of Surgical Sciences, University of Turin, Via Genova 3, Turin 10126, Italy. [marcogatti17@gmail.com](mailto:marcogatti17@gmail.com)

### Abstract

Liver lesions are common findings in radiologists' daily routine. They are a complex category of pathology that range from solitary benign lesions to primary liver cancer and liver metastases. Benign focal liver lesions can arise from different liver cell types: Epithelial (hepatocytes and biliary cells) and none-pithelial (mesenchymal cells). Liver magnetic resonance imaging (MRI) is a fundamental radiological method in these patients as it allows with its multiparametric approach optimal non-invasive tissue characterization. Furthermore, advanced liver MRI techniques such as diffusion-weighted imaging and hepatobiliary contrast agents have improved the detection of focal liver lesions and can be highly effective in differentiating pseudotumor from tumors, as well as benign from malignant lesions, and can also be used for differential diagnosis. Although histological examination can be useful in making a definitive diagnosis, MRI is an important modality in the diagnosis of liver lesions with a significant impact on patient care. This aim of this review is to provide a comprehensive overview of benign liver lesions on MRI.

**Key Words:** Magnetic resonance imaging; Liver neoplasms; Biliary tract; Hepatocytes

**Core Tip:** Liver magnetic resonance imaging (MRI) is a fundamental radiological technique in patients with focal liver lesions as it allows, with its multiparametric approach, optimal non-invasive tissue characterization. Liver MRI can be highly effective in distinguishing pseudotumor from tumors, as well as benign from malignant lesions and can also be used for differential diagnosis. Although histopathological assessment sometimes has an important role in definitive diagnosis, MRI is a key imaging modality in the diagnosis of liver lesions with a great impact on patient management.

**Citation:** Gatti M, Maino C, Tore D, Carisio A, Darvizeh F, Tricarico E, Inchingolo R, Ippolito D, Faletti R. Benign focal liver lesions: The role of magnetic resonance imaging. *World J Hepatol* 2022; 14(5): 923-943

**URL:** <https://www.wjgnet.com/1948-5182/full/v14/i5/923.htm>

**DOI:** <https://dx.doi.org/10.4254/wjh.v14.i5.923>

## INTRODUCTION

Liver lesions are common findings in radiologists' daily routine. They are a complex category of pathology that ranges from solitary benign lesions to primary liver cancer and liver metastases[1-4]. Benign focal liver lesions can arise from different liver cell types: Epithelial (hepatocytes and biliary cells) and nonepithelial (mesenchymal cells)[5]. The diagnosis is often straightforward, although sometimes distinguishing between malignant primary and secondary lesions may represent a diagnostic challenge due to atypical tumor appearance and features.

To avoid misdiagnosis, radiologists must cope with the key characteristics of the lesion and decide which imaging procedure [*i.e.*, ultrasound (US), computed tomography (CT) and/or magnetic resonance imaging (MRI)] will most likely provide the diagnosis[3,4,6-8].

The use of advanced liver MRI techniques such as diffusion-weighted imaging (DWI), multiarterial phase technique, hepatobiliary contrast agents and artificial intelligence have improved the detection and differentiation of different focal liver lesions[2-4,8-11]. Furthermore, liver MRI is often the last imaging technique used in the diagnostic algorithm before liver biopsy.

Therefore, it is important to know the characteristics of different focal liver lesions on MRI and how to differentiate between benign and malignant lesions in order to make the correct diagnosis, recommend the best follow-up when necessary, cut the costs of unnecessary diagnostic tests and, last but not least, reduce patient anxiety.

This aim of this article is to provide a comprehensive overview of benign liver lesions on MRI. A schematic representation showing MRI features of benign liver lesions is presented in Figure 1. Table 1 shows the histological classification that was used in this review. Table 2 provides an overview of the MRI contrast agents currently used in clinical practice.

## EPIHELIAL TUMORS (HEPATOCELLULAR AND BILIARY)

### Hepatocellular adenoma

Hepatocellular adenoma (HCA) is a rare benign monoclonal neoplasm of the liver, composed of hepatocytes arranged in sheets or in a cord-like fashion with a lack of portal venules and biliary ductules[12-14]. Hepatocyte sheets are separated by dilated sinusoids. They are perfused solely by high-pressure peripheral arterial feeding vessels, resulting in a remarkable hypervascular nature. Hepatocytes might contain a variable amount of intracellular fat or glycogen.

HCA has an annual incidence of about 1-1.3 million cases per year in North America and Europe; 85% of cases occur in women of childbearing age (15-45 years old)[15]. An increased incidence of HCAs has been reported since the 1960s following the introduction of oral contraceptive pills (OCPs)[14,16]: Long-term users of OCPs have a 25-fold increased risk of developing HCA compared to the general population[14]. Some studies suggested that OCP discontinuation might lead to tumor regression, but this remains controversial[17]. Similarly, long-term use of anabolic androgen steroids (AAS) has been associated with a high risk of developing HCA. Glycogen storage disorders (GSDs), in particular type 1 and type 3, have been linked to an increased incidence of HCAs[14].

Hepatic adenomatosis, first described in 1985, is a condition in which 10 or more adenomas are present in an otherwise normal liver[18]. These cases are at higher risk of complications: 63% risk of hemorrhage and 10% risk of malignant transformation[19]. Other risk factors for HCA are diabetes (both type 1 and 2), metabolic syndrome, obesity, Fanconi's anemia, familial adenomatous polyposis,

**Table 1 Histological classification of benign liver lesions**

Epithelial tumors (hepatocellular and biliary)	Mesenchymal tumors	Pseudotumor
Hepatocellular adenoma	Hemangioma	Focal fatty infiltration
Focal nodular hyperplasia	Lymphangioma	Infection (liver abscess, <i>Echinococcus granulosus</i> )
Biliary cystadenoma	Solitary fibrous tumor	Inflammatory disorder of the liver (pseudotumor, sarcoidosis)
Biliary hamartoma (von Meyenburg Complex)	Mesenchymal hamartoma	

**Table 2 Magnetic resonance contrast agent**

Category	Molecule	Structure	Ioniity	Relaxivity	Recommended dose (mmol/kg)	Excretion
ECAs	Gadoterate meglumine (Dotarem)	Macroyclic	Ionic	Standard	0.1	Renal
ECAs	Gadobutrol (Gadavist)	Macroyclic	Non-ionic	Standard	0.1	Renal
ECAs	Gadoteridol (Prohance)	Macroyclic	Non-ionic	Standard	0.1	Renal
ECAs	Gadopentetate dimeglumine (Magnevist)	Linear	Ionic	Standard	0.1	Renal
ECAs	Gadoversetamide (OptiMark)	Linear	Non-ionic	Standard	0.1	Renal
ECAs	Gadodiamide (Omniscan)	Linear	Non-ionic	Standard	0.1	Renal
HBA	Gd-EOB-DTPA (Eovist/Primovist)	Linear	Ionic	High	0.025	50% renal, 50% biliary
HBA	Gd-BOPTA (MultiHance)	Linear	Ionic	High	0.1	5% biliary, 95% renal
BPA	Gadofosveset trisodium (Ablavar)	Linear	Ionic	High	0.03	Renal

ECAs: Extracellular agents; HBA: Hepatobiliary agents; BPA: Blood pool agents.

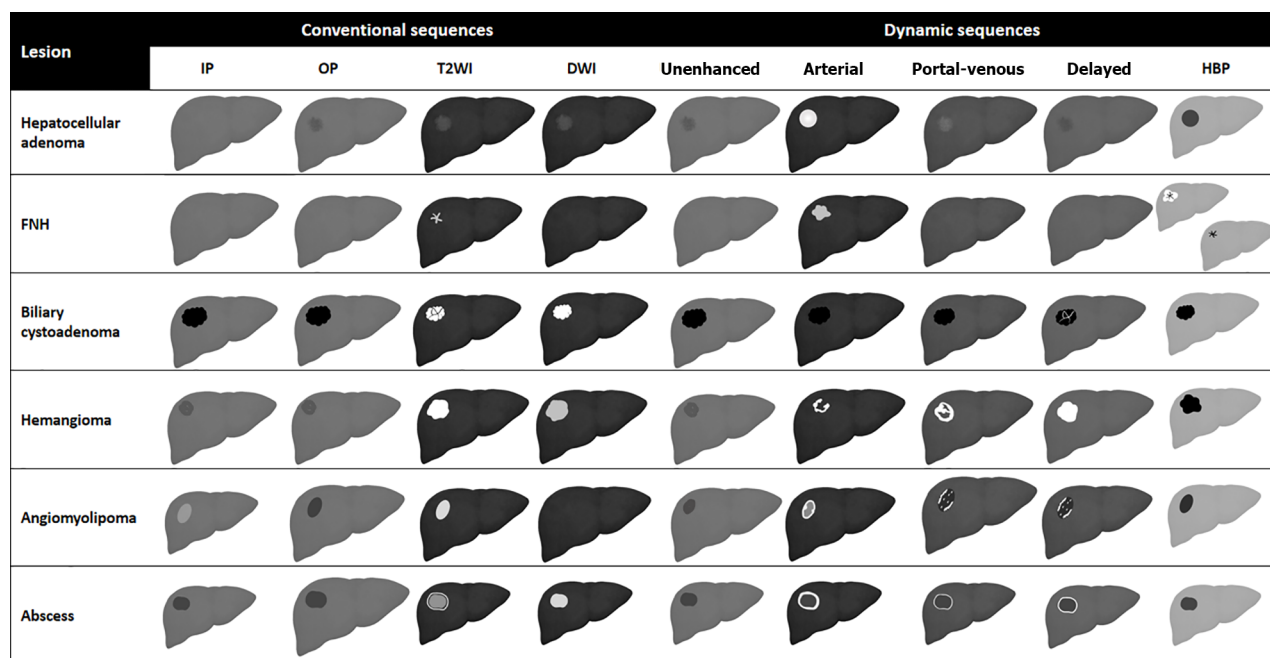


**Figure 1 Schematic representation showing liver magnetic resonance imaging features of benign liver lesions.** IP: T1-weighted in-phase imaging; OP: T1-weighted out-of-phase imaging; DWI: Diffusion weighted imaging; HBP: Hepatobiliary phase; FNH: Focal nodular hyperplasia.

beta thalassemia and tyrosinemia[14].

HCA may be complicated by the presence of intralesional fat, hemorrhage, or malignant transformation with a subsequent wide range of imaging appearances resulting in a challenging diagnostic process. In 2006, four subtypes of HCA were identified based on genotype-phenotype analyses according to the genetic and histopathological features of the lesion: (1) Type 1: Hepatocyte nuclear factor (HNF)-1 $\alpha$  HCA; (2) Type 2: Inflammatory HCA (I-HCA); (3) Type 3:  $\beta$ -catenin activated

HCA; and (4) Type 4: Unclassified HCAs[12].

Several hypervascular benign and malignant hepatic lesions may mimic HCA: Focal nodular hyperplasia (FNH), hepatocellular carcinoma (HCC), hemangioma (HA), angiomyolipoma and metastases. The use of hepatocyte-specific contrast agent allows differential diagnosis between HCA and FNH with very high sensitivity and specificity (respectively 91% to 100% and 87% to 100%)[20]. On the hepatobiliary phase (HBP), most HCAs present a low signal compared to surrounding parenchyma, while FNHs have an iso- or hyperintense signal. Some HCAs, however, generally I-HCAs, may have an iso- or hyperintense signal on the HBP.

#### Type 1: HNF-1 $\alpha$ HCA

HNF-1 $\alpha$  HCA is the second most common subtype of HCA, representing 30% to 35% of lesions; it is almost exclusively found in women, the majority of whom (> 90%) with a history of OCP use in anamnesis[20]. This type of HCA may be associated with maturity-onset diabetes of the young and familial adenomatosis. HNF-1 $\alpha$  HCA generally has an indolent biological behavior and among all types of HCA it has the lowest risk of malignant degeneration. HNF-1 $\alpha$  HCA may be associated with mutations of the transcription factor 1 gene on chromosome 12q24.43, an anti-oncogene involved in hepatocyte differentiation, whose inactivation can promote proliferation of such cell lines[14].

Due to its intracellular fat content, HNF-1 $\alpha$  HCA typically exhibits diffuse intratumoral signal loss on chemical-shift T1-weighted imaging (*i.e.*, signal loss on opposed-phased images compared to in-phase images); this finding alone demonstrates 86.7% sensitivity and 100% specificity for this subtype. HNF-1 $\alpha$  HCA is often hyper- or iso-intense on T1-weighted images and iso- or hyperintense on T2-weighted images, with no apparent signal restriction on diffusion imaging. HNF-1 $\alpha$  HCAs often show hyper-enhancement in the arterial phase after contrast injection; however, this does not persist in the portal venous phase[14,21] (Figure 2).

#### Type 2: I-HCA

This is the most frequent subtype, accounting for 40% to 50% of all HCAs; it is linked to mutations in the interleukin 6 signal transducer gene, which is located on chromosome 5q11 and codes for glycoprotein 130. This mutation causes the Janus kinase (JAK) signal transducer to be activated indefinitely, resulting in aberrant hepatocyte proliferation. Type 2 HCA is most common in young women on OCP medication, as well as in those with metabolic syndrome or obesity.

I-HCA is the HCA type with the highest risk of bleeding, occurring in up to 30% of cases. Malignant transformation of HCAs into HCC occurs in 5% to 10% of cases. On MRI, I-HCA generally shows a heterogeneous high signal on T2-weighted sequences, more intense in the peripheral part of the lesion ("atoll" sign) and arterial enhancement that persists in the portal venous and delayed phases. Such features are due to the presence of dilated sinusoids. Intralesional steatosis is rare, more frequently focal or with a patchy and heterogeneous pattern. Intratumoral hemorrhage, reported in up to 30% of cases, results in increased lesion heterogeneity (Figure 3). Acute hemorrhage presents a high signal on T1-weighted sequences due to the presence of methemoglobin; chronic hemorrhage has a low signal on T1 and T2-weighted sequences due to hemosiderin content[14,21].

#### Type 3: $\beta$ -catenin-activated HCA

$\beta$ -catenin activated HCAs account for 10% to 15% of all HCAs. Mutations in the  $\beta$ -catenin gene (CTNNNB1) on chromosome 3p21 cause continuous activation of the  $\beta$ -catenin protein, resulting in uncontrolled hepatocyte growth. It is more common in men and is linked to GSDs, AAS, and familial adenomatous polyposis.  $\beta$ -catenin mutation is strongly associated with malignant degeneration[14].

$\beta$ -catenin-activated HCAs do not have typical MRI features. Such lesions generally do not contain intratumoral fat. Malignant transformation may be suspected in the case of growth, local invasion, or contrast medium washout on portal-venous or delayed phases.  $\beta$ -catenin-activated HCAs present arterial enhancement and washout on the portal-venous and delayed phase, making differential diagnosis with HCC challenging[14,21,22].

#### Type 4: Unclassified HCAs

This category includes approximately 10% of all HCAs with an adenoma-like appearance but no distinguishing genetic and/or clinical characteristics. There is a scarcity of information about these lesions. Such tumors have no pathognomonic characteristics on MRI[14,23].

#### FNH

After HA, FNH is the second most common benign hepatic tumor (representing around 8%-9% of all primary liver tumors) and is frequently an incidental finding on imaging as most individuals are asymptomatic. FNHs are more common in females than in males (8:1), in the third to fifth decades, and, unlike HCAs, a relationship with OCPs is uncommon. Severe FNH syndrome is defined as the presence of multiple FNH lesions (up to 20%) and HAs. To ensure adequate treatment, it is crucial to distinguish FNH from other hypervascular liver lesions such as HCA, HCC, and hypervascular metastases[24].

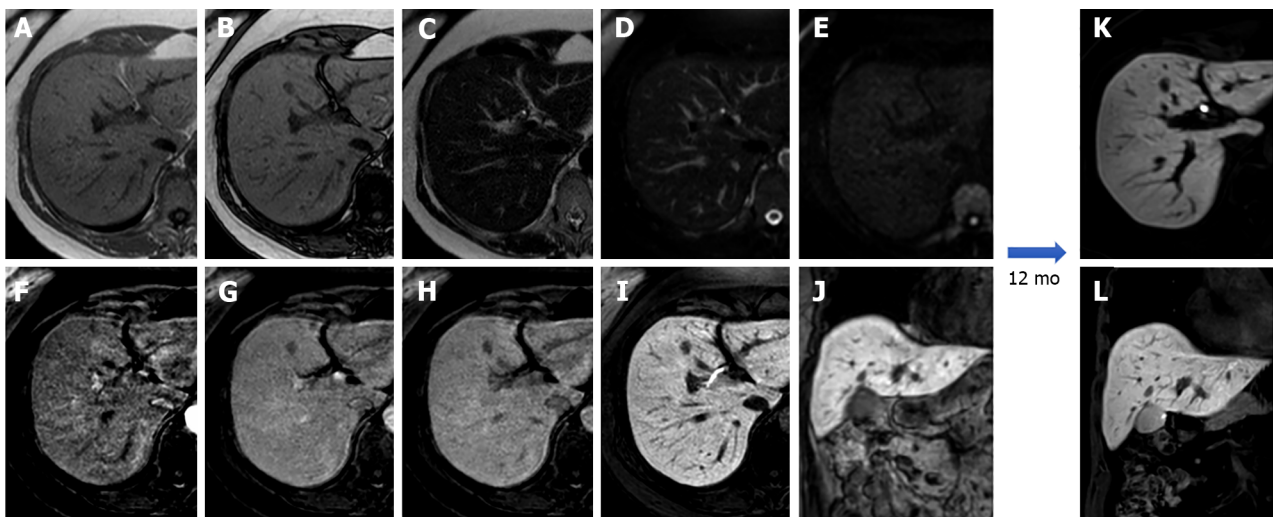


**Figure 2** A 53-year-old patient presented with right hypochondrium pain and underwent abdominal ultrasound examination demonstrating a hyperechoic nodule in S4. Liver magnetic resonance imaging confirmed an isointense nodule on T1 in-phase sequence with loss of signal on opposed-phase T1-weighted images, isointense on T2 sequences, without increased signal intensity on diffusion weighted images, with minimum wash-in on the arterial phase and wash-out on the portal-venous and delayed phase, hypointense in the hepatobiliary phase, findings consistent with hepatocyte nuclear factor 1 $\alpha$ -mutated hepatocellular adenoma. A: In-phase T1-weighted image; B: Out-of-phase T1-weighted image; C: T2-weighted image; D: T2-Spectral Attenuated Inversion Recovery; E: High  $b$ -value diffusion weighted imaging; F: Arterial phase magnetic resonance imaging (MRI); G: Portal venous phase MRI; H: Delayed phase MRI; I-L: Hepatobiliary phase MRI.

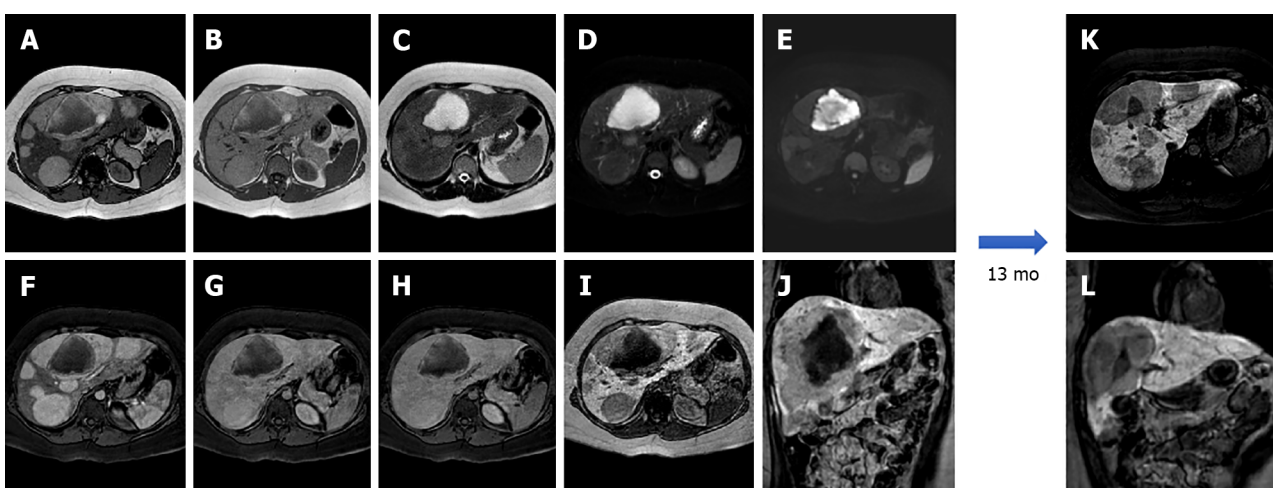


**Figure 3** A 25-year-old female with 10-year history of oral contraceptive pill presented to the emergency department with diffuse abdominal pain. Liver magnetic resonance imaging demonstrated multiple hepatic lesions, the larger 15 cm in diameter in S4-S5-S8 shows iso-hyperintense signal on T1-weighted sequences, with dishomogenous hypointense central component with peripheral hyperintensity. The lesion is isointense on T2-weighted sequences with marked hyperintensity of the central component; on diffusion weighted images the mass presents a slight increase in signal while the central portion has a marked signal increase. At the dynamic study, the mass has wash-in that persists on the portal venous and delayed phase while the central portion illustrates minimum enhancement. The mass is hypointense on the hepatobiliary phase with a marked hypointense central portion. Liver biopsy demonstrated a hepatic adenoma with a bleeding component. At 13 mo follow-up, the lesion presented a slightly reduced diameter while the central bleeding component was almost completely reabsorbed. A: Out-of-phase T1-weighted image; B: In-phase T1-weighted image; C: T2-weighted image; D: T2-Spectral Attenuated Inversion Recovery; E: High  $b$ -value diffusion weighted imaging; F: Arterial phase magnetic resonance imaging (MRI); G: Portal venous phase MRI; H: Delayed phase MRI; I-L: Hepatobiliary phase MRI.

FNH should be regarded as a regenerative lesion rather than a neoplasm: It may be caused by the presence of a vascular abnormality (either of the arterial or portal vascular supply) that, when combined with hormonal stimulation, results in mass growth. Histologically, these lesions are known as hamartomatous malformations[25]. From an anatomopathological point of view FNH is a nodule with polycyclic contours, composed of organized hepatocytes, completely or incompletely surrounded by circular or short fibrous septa originating from a central scar that contains a hypertrophic arterial vessel, originating from the hepatic artery.

The surrounding septa connective tissue also contains numerous capillaries and ductules. The rich network of capillaries, that arise from the central artery, provide arterial blood to the hepatocytes and sinusoids, in accordance with the highly hypervascular nature of most FNH lesions on imaging[26]. The sinusoids, the malformed arteries and the vein of FNH drain into the hepatic vein. FNH does not have a portal venous supply. Normal liver tissue surrounds the FNH and there is no fibrous capsule at the interface of the lesion and the liver[27].

Due to its vascular physiopathology, FNH is commonly associated (20%-30%) with other hepatic lesions or conditions such as hepatic HA, arteriovenous malformations, anomalous venous drainage, HCA (possible but not proven), congenital absence of portal vein/portal vein atresia and portal shunts [28]. Because it contains hepatocytes, FNH shows an isointense signal on both T1- and T2-weighted sequences with occasional slight hypointensity and hyperintensity on T1 and T2, respectively.

MRI imaging has higher sensitivity (70%) and specificity (98%) for FNH than US and CT. Both on CT and MRI, after contrast medium administration, FNH shows homogenous and strong contrast enhancement in the arterial phase with the exception of the central scar[26]. During portal-venous and delayed phases, it becomes isointense to the liver parenchyma while the central scar remains relatively hypointense. On HBP FNH appears isointense to hyperintense compared to adjacent liver parenchyma without or with the presence of a central scar[21], which is hypointense (Figure 4).

On diffusion weighted imaging the average numerical value of the apparent diffusion coefficient (ADC) in benign hepatic lesions (FNH, HA, HCA) is about  $1.88 (1.326-2.48) \times 10^3 \text{ mm}^2/\text{s}$ , while the ADC of malignant liver lesions [HCC, cholangiocarcinoma (CCC), colorectal cancer liver metastasis (CRCLM)] are significantly lower, around  $1.15 (1.024-1.343) \times 10^3 \text{ mm}^2/\text{s}$ [29]. FNH and HCA have ADC values lower than normal liver but FNH has an ADC higher than HCA[30].

The central scar is more often detected with MRI than with CT (78% and 60%, respectively)[31]. The central scar appears slightly hyperintense on T2-weighted images and this is an important difference compared with the central scar of HCC that is generally hypointense in all sequences and is rarely hyperintense, mimicking that of FNH[32].

On MRI with non-hepatobiliary specific agents (and consequently also on CT imaging) the central scar shows enhancement in the delayed phase due to the presence of abundant myxomatous stroma. With different hepatobiliary specific agents the central scar manifests variously[32]: (1) With gadobenate dimeglumine (Gd-BOPTA - MultiHance®; Bracco, Milan, Italy) the central scar will enhance in the late phase (hepato-biliary excretion after 1-3 h); and (2) With gadoxetic acid (Gd-EOB-DTPA - Primovist®; Bayer-Schering, Berlin, Germany) the central scar will never enhance because the late venous phase overlaps the HBP (that comes on average after 10-100 min) making everything that is not of hepatocellular origin hypointense, including the connective central scar.

### **Atypical FNH**

Currently, FNH is divided into two types: Classic and non-classic. Classic FNH is characterized microscopically by the presence of: (1) Abnormal nodular architecture; (2) Malformed vessels; and (3) Cholangiolar proliferation and on imaging appears with all the characteristics mentioned above. Non-classic FNH lesions lack one of the classic features but always show bile ductular proliferation[24]. Non-classic FNH may demonstrate “atypical appearance” at imaging that may lead to the following 5 subtypes: (1) No central scar FNH; (2) Large central scar; (3) Intralesional fat; (4) Presence of a pseudo-capsule; and (5) Sinusoidal distension (Figure 5).

### **Biliary cystadenoma**

Biliary cystadenoma (BCA) is an uncommon (less than 5% of cystic liver lesions) benign hepatic tumor that arises from intrahepatic biliary channels, most commonly in the right lobe (55%), and rarely from extrahepatic biliary ducts or the gallbladder[33]. Due to its high prevalence in middle-aged women (> 85%)[33] it is considered a congenital disorder with potential hormonal influence. Due to its high risk of recurrence (if non-completely removed) and its potential risk for malignant degeneration into biliary cystadenocarcinoma (BCAC), the differential diagnosis with other cystic lesions of the liver is mandatory[21].

US imaging reveals a massive, lobulated, well-defined hypoechoic or anechoic mass with hyperechoic interior septa or calcifications and solid papillary projections; contrast-enhanced ultrasonography (CEUS) may indicate enhancement of the walls and septa. These features may aid in identifying BCA from other liver cystic lesions[33].

CT confirms US appearance and CEUS behavior: A single multiloculated cystic lesion with a well-defined thick fibrotic capsule, mural nodules, and rarely calcifications of the capsule[33]. On MRI, BCA appears as a fluid-containing multilocular lesion that is significantly hypointense on T1-weighted sequences and hyperintense on T2-weighted images with septal hypointensity. On both T1- and T2-weighted images, the signal intensity may fluctuate due to the presence of proteinaceous material or blood products[21] (Figure 6). If thinner septa and a regular wall are seen in cystadenoma, polypoid excrescences, hemorrhage and evident vascularized septa are more suspicious for BCAC, but the differential diagnosis between such lesions may be challenging[21].

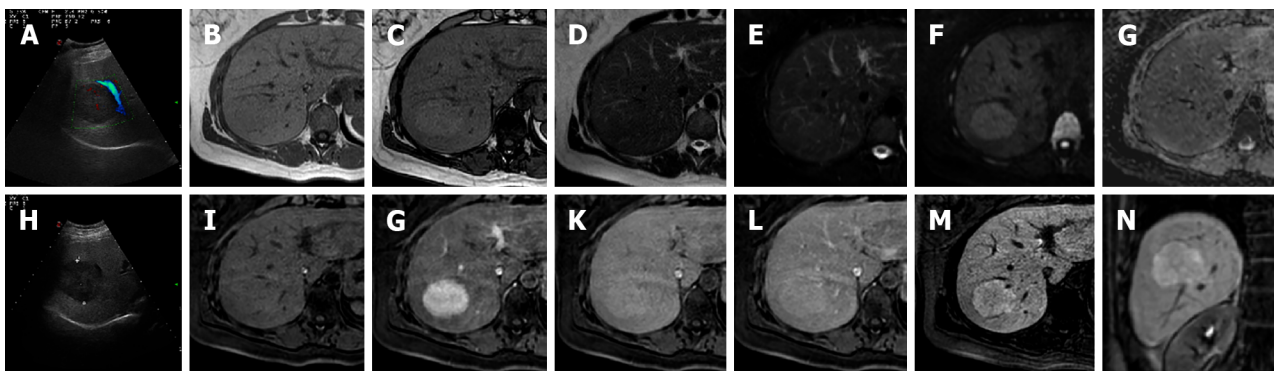


**Figure 4** A 41-year-old female presented to the emergency department with diffuse abdominal pain and underwent ultrasound examination revealing a 5.3 cm solid hypoechoic lesion in S7. Liver magnetic resonance imaging confirmed an isointense lesion on T1-weighted sequence, isointense in T2 sequences, with minimum increased signal intensity on diffusion weighted images and isointense on the ADC map. After gadoxetic acid administration the lesion shows intense arterial enhancement; slightly hyperintense on the portal venous and delayed phases. The mass shows hyperintense signal on the hepatobiliary phase. These findings are consistent with typical focal nodular hyperplasia. A: Liver ultrasound image; B: In-phase T1-weighted image; C: Out-of-phase T1-weighted image; D: T2-weighted image; E: T2-Spectral Attenuated Inversion Recovery; F: High *b*-value diffusion weighted imaging; G: ADC map; H: Liver ultrasound image; I: Pre-contrast phase magnetic resonance imaging (MRI); J: Arterial phase MRI; K: Portal venous phase MRI; L: Delayed phase MRI; M and N: Hepatobiliary phase MRI.

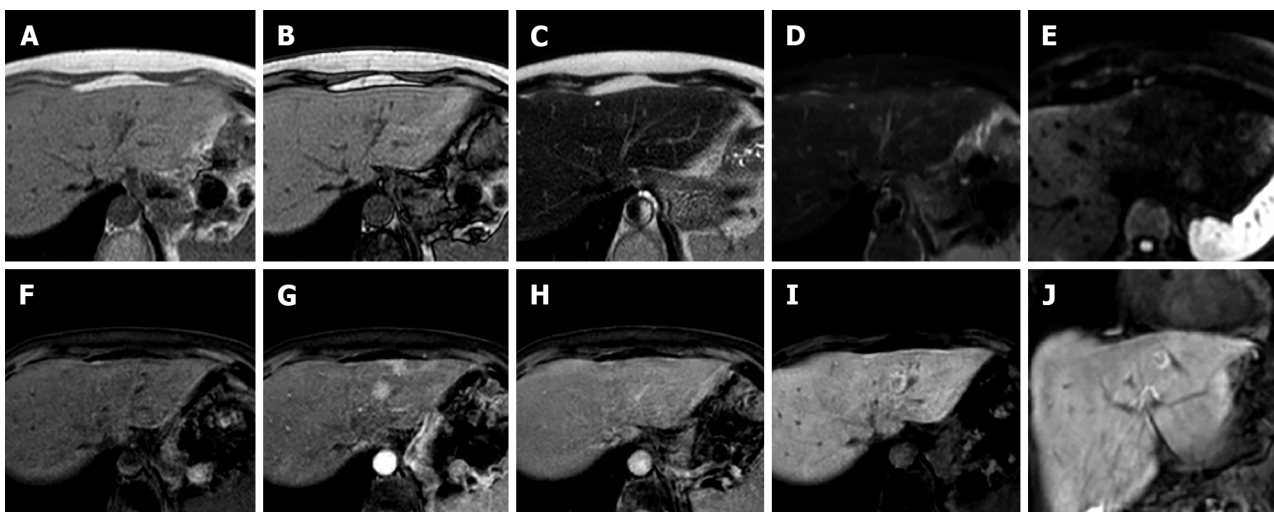


**Figure 5** A 56-year-old female with ultrasound evidence of a hyperechoic nodular lesion in S8. Liver magnetic resonance imaging confirmed a nodule, slightly hypointense on T1-weighted, slightly hyperintense on T2-weighted sequences, without increased signal intensity on diffusion weighted images. After gadoxetic acid administration, the lesion shows homogeneous arterial enhancement, becomes isointense during the portal venous phase, and presents peripheral hyperintensity with a hypointense core on the hepatobiliary phase. Such findings are consistent with atypical focal nodular hyperplasia. A: In-phase T1-weighted image; B: Out-of-phase T1-weighted image; C: T2-weighted image; D: T2-Spectral Attenuated Inversion Recovery; E: High *b*-value diffusion weighted imaging; F: Pre-contrast phase magnetic resonance imaging (MRI); G: Arterial phase MRI; H: Portal venous phase MRI; I and J: Hepatobiliary phase MRI.

### Biliary hamartoma (von Meyenburg Complex)

Multiple biliary hamartomas, also known as von Meyenburg Complex, are rare bile duct malformations, with a very low incidence ranging between 0.4% and 5.5%. There is a higher prevalence in females (F/M = 7/4) with a mean age of 48 years (range 33-68 years). They belong to the spectrum of "fibropolycystic liver disease" and are defined as small duct dilatations within thick bile. The cause is unknown, however it can be present in both non-cirrhotic and cirrhotic livers, as well as in children and adults. However, its prevalence rises dramatically with chronic liver illness, implying an acquired etiology[34].

Histologically, bile duct hamartomas are generally small, less than 1 cm, often subcapsular, and composed of small dilated biliary ducts surrounded by biliary epithelium[35]. On T1-weighted images they typically appear as small hypointense lesions, with a strongly increased signal on T2WI due to its intrinsic cystic component especially on heavily weighted T2 sequences. These lesions can show the presence of small mural nodules (1-2 mm) with an isointense signal on T1-weighted and an intermediate signal on T2-weighted images. On dynamic sequences, the mural nodules can show enhancement during the portal-venous phase in about 90% of cases with no core enhancement. On cholangiography sequences, both intra- and extra-hepatic bile ducts are normally represented[36,37],

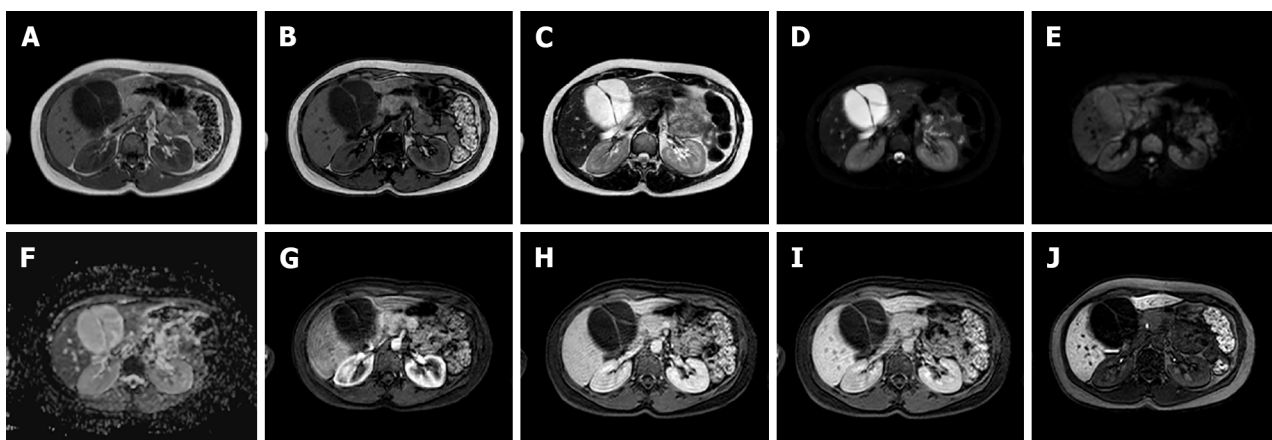


**Figure 6 A 34-year-old female patient.** Liver magnetic resonance imaging demonstrated a multiloculated cystic mass in S4b, hypointense on T1 sequences with isointense septa, hyperintense on T2 sequences, slightly hyperintense on diffusion weighted images and without significant restriction on the ADC map. On dynamic study after gadoxetic acid administration, the lesion presents no enhancement even in the septal components. On the hepatobiliary excretion phase the mass is hypointense. After surgical resection, histological examination demonstrated a biliary cystadenoma. A: In-phase T1-weighted image; B: Out-of-phase T1-weighted image; C: T2-weighted image; D: T2-Spectral Attenuated Inversion Recovery; E: High *b*-value diffusion weighted imaging; F: ADC map; G: Arterial phase magnetic resonance imaging (MRI); H: Portal venous phase MRI; I: Delayed phase MRI; J: Hepatobiliary phase MRI.

while multiple hyperintense cystic lesions on T2-weighted images are uniformly distributed in the liver with no communication with the bile ducts, appearing as a “starry sky” configuration[38] (Figure 7). Biliary hamartomas should be carefully recognized in order to distinguish it from metastases, microabscess, simple liver cysts, and Caroli disease (Figure 8).

## MESENCHYMAL TUMORS

### HA

Hepatic HAs are the most prevalent benign mesenchymal liver lesions, with an estimated frequency of around 20% in the general population, and are up to five times more common in females than males [39]. HAs are frequently an incidental finding in asymptomatic patients during routine radiological examinations; however, because of their high prevalence, the differential diagnosis can become complex in patients affected by primary liver cancer or liver metastases. HAs are categorized by size: Small HAs are 1-2 cm, typical HAs are 2-10 cm and giant HAs have a diameter of more than 10 cm. Recent retrospective cohort studies demonstrated that up to 40% of HAs may grow during follow-up, with a slow growth rate (2 mm/year in diameter and 17.4%/year in volume)[39].

Microscopically, HAs appear as cavernous vascular spaces lined by endothelium and containing a fibrous stroma. Larger HAs may contain a fibrous nodule or a collagen scar. HAs are usually fed by vessels from the hepatic artery circulation, with a slow blood flow within the vascular spaces. HAs have been histologically categorized in 3 different subtypes, with some overlap among them: Cavernous, capillary and sclerosed.

#### Cavernous HA

This is the most common subtype, generally smaller than 3 cm with few internal connective components and with a prevalence of large vascular spaces[21]. The high water content of HAs causes homogeneous hyperintensity on T2-weighted sequences and poor signal intensity on T1-weighted images during MRI [40]. Giant HAs may present a central T2-weighted hypointense component in the case of hyalinized or thrombosed areas. If calcifications are present, they show very low signal intensity on all sequences.

On diffusion weighted imaging, HAs show hyperintensity on  $b$  0 s/mm<sup>2</sup> images, with a progressive decrease in signal intensity at higher  $b$  values; the signal on the ADC map is greater than that of the nearby liver parenchyma. Some HAs have residual hyperintensity on high  $b$  value images (500-750 s/mm<sup>2</sup>) because of the “T2 shine through effect” making them more difficult to characterize; however, quantitative assessment with the ADC map make differential diagnosis easy as their signal is always higher than that of surrounding liver[41]. Following contrast injection, typical cavernous HAs exhibit peripheral nodular enhancement on the arterial phase, with centripetal progression and progressive filling on the portal venous and delayed phases; due to a lack of hepatocytes, they display a hypointense signal on the HBP[21] (Figure 9).

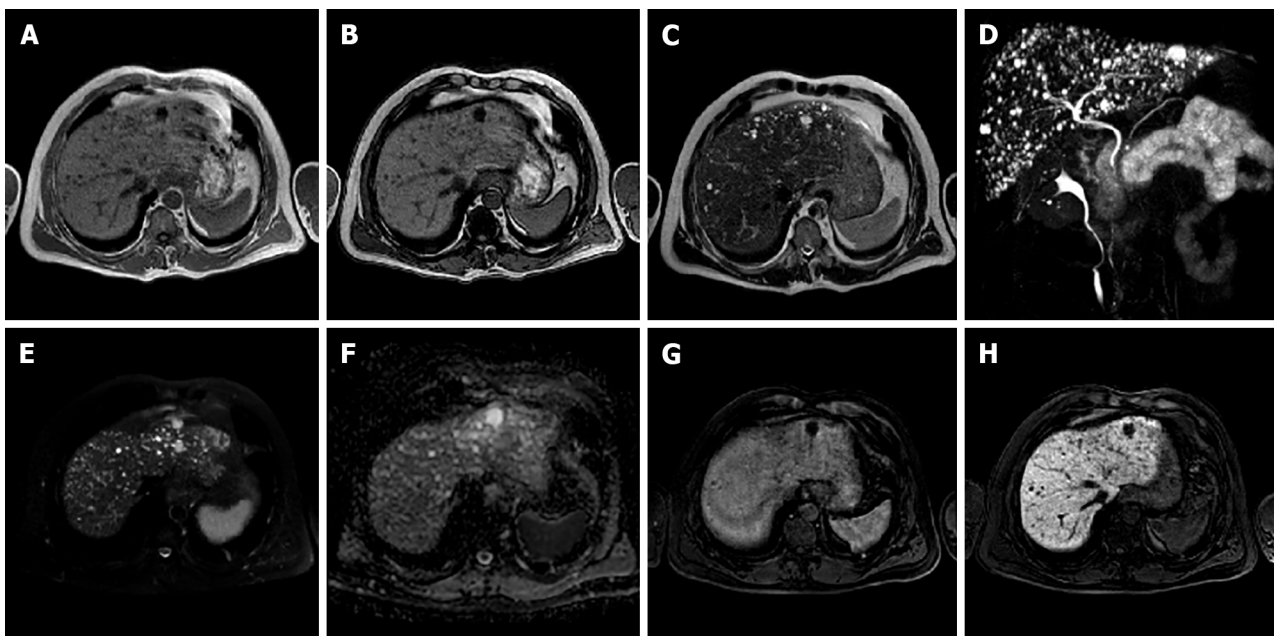


**Figure 7 A 50-year-old male.** Liver magnetic resonance imaging demonstrates the presence of multiple bilobar small nodular lesions, hypointense on T1 imaging, hyperintense on T2 sequences, without diffusion restriction on the ADC map and presenting no enhancement on the portal venous phase after contrast injection. These nodules are hypointense on the hepatobiliary phase. Such features and the lack of communications with the biliary tree demonstrated on maximum intensity projection images from magnetic resonance cholangiography are consistent with multiple biliary hamartomas (von Meyenburg complex). A: In-phase T1-weighted image; B: Out-of-phase T1-weighted image; C: T2-weighted image; D: 3D maximum intensity projection reconstruction magnetic resonance cholangiopancreatography; E: High *b*-value diffusion weighted imaging; F: ADC map; G: Portal venous phase magnetic resonance imaging (MRI); H: Hepatobiliary phase MRI.

### Capillary HA

This accounts for almost 16% of all HAs, being smaller than 1 cm in about 40% of cases[42,43]. Microscopically it consists of small vascular spaces with abundant connective components. It presents high signal intensity on T2-weighted images and low signal intensity on T1-weighted sequences. In the case of hepatic steatosis, it shows a hyperintense signal on T1-weighted “chemical shift” images due to peritumoral sparing of fatty infiltration.

After contrast injection it is characterized by a “flash-filling” kinetic of contrast enhancement with early homogeneous enhancement, similar to that of the aorta in all phases[21]. Due to the presence of arterioportal shunts, fugacious perilesional parenchymal enhancement may be observed in extremely tiny lesions (less than 1 cm). Relative hyperintensity on delayed phases allows differential diagnosis with hypervascular metastases that are hypointense in the portal venous and delayed phases.

### Sclerosed/hyalinized HA

Sometimes HAs deteriorate, resulting in the development of severe fibrosis, which usually begins at the core of the lesion, obliterating vascular gaps and causing changes in MRI signal intensity. Sclerosed HAs may only present slight hyperintensity on T2-weighted images, generally localized at the periphery of the lesion. Owing to histologic lesion heterogeneity, the contrast enhancement pattern may be unusual. In most cases no early enhancement is present and there is a slow and inhomogeneous contrast progression. Late centripetal filling of the central scar might be present. Due to its rarity and heterogeneous radiological presentation, that can mimic hepatic malignancies such as CCC or metastases, the final diagnosis of sclerosed HA is often histological[8,21,42,44] (Figure 10).

### Angiomyolipoma

Hepatic angiomyolipomas (HAMLs) are mesenchymal benign tumors composed of arteries, fat, and smooth muscle cells that are categorized into four subtypes based on their composition: Mixed (the most frequent form), lipomatous (containing 70% fat), myomatous (containing 10% fat), and angiomatous.

The fat components of a lesion might range from 10% to > 90% of the total lesion volume. Patients with tuberous sclerosis complex are more likely to have these tumors (5%-10% of the time)[45]. HAML is classified as a “Perivascular Epithelioid Cell Tumor” and is immunohistochemically positive for beta-hydroxy-beta-methylbutyrate-45, a monoclonal antibody for melanoma: This positivity is a clear diagnostic criterion, while other hepatic tumors are negative for this marker.

The radiological appearance of HAML is completely dependent on the proportions of these three components. Lipomatous HAML appear hyperechogenic on US, hypodense on non-contrast enhanced CT, hyperintense on in-phase T1-weighted sequences, and hypointense on out-of-phase T1-weighted

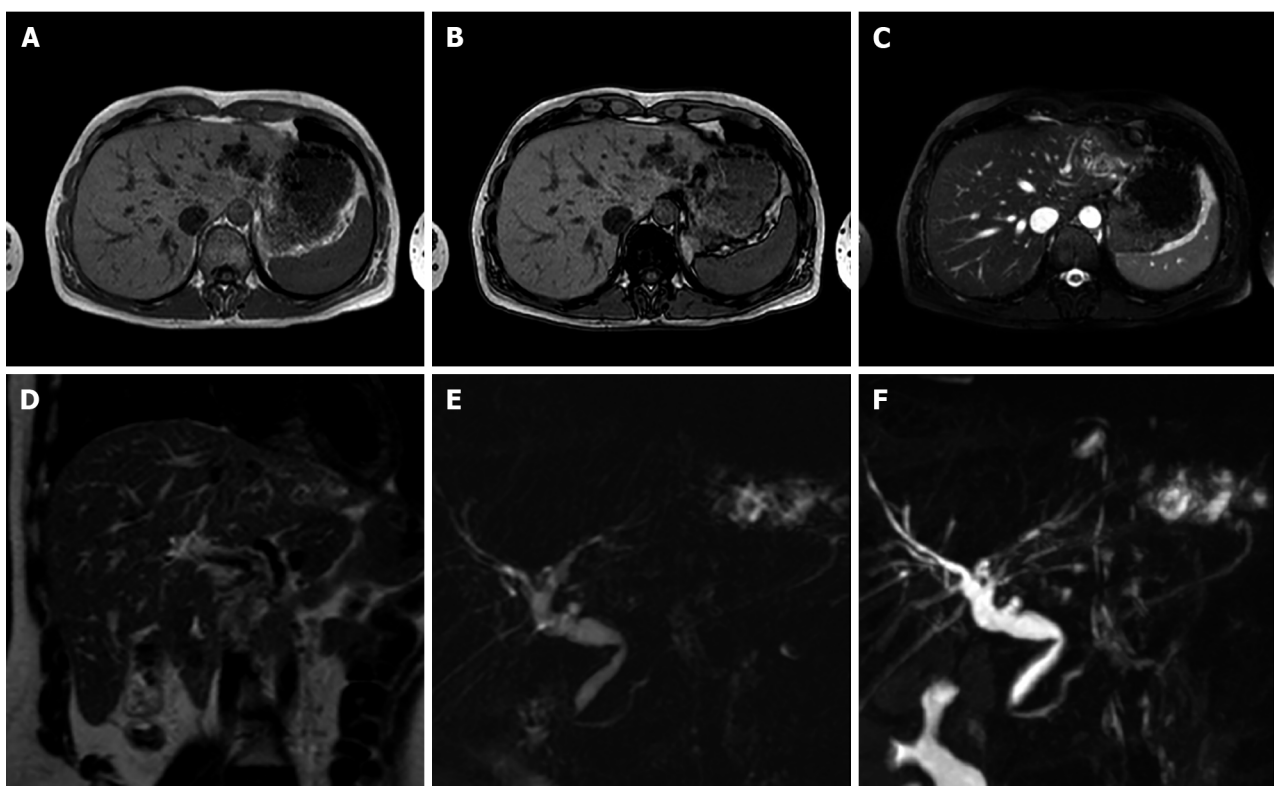


**Figure 8 A 40-year-old female.** Liver magnetic resonance imaging demonstrates dilatation of the left biliary hemisystem with multiple voids of signal on long TR sequences compatible with lithiasis. Pathology examination after left hepatectomy confirmed Caroli disease. A: In-phase T1-weighted image; B: Out-of-phase T1-weighted image; C: T2-Spectral Attenuated Inversion Recovery; D: T2-weighted image; E: Single-shot magnetic resonance (MR) cholangiopancreatography; F: 3D maximum intensity projection reconstruction MR cholangiopancreatography.

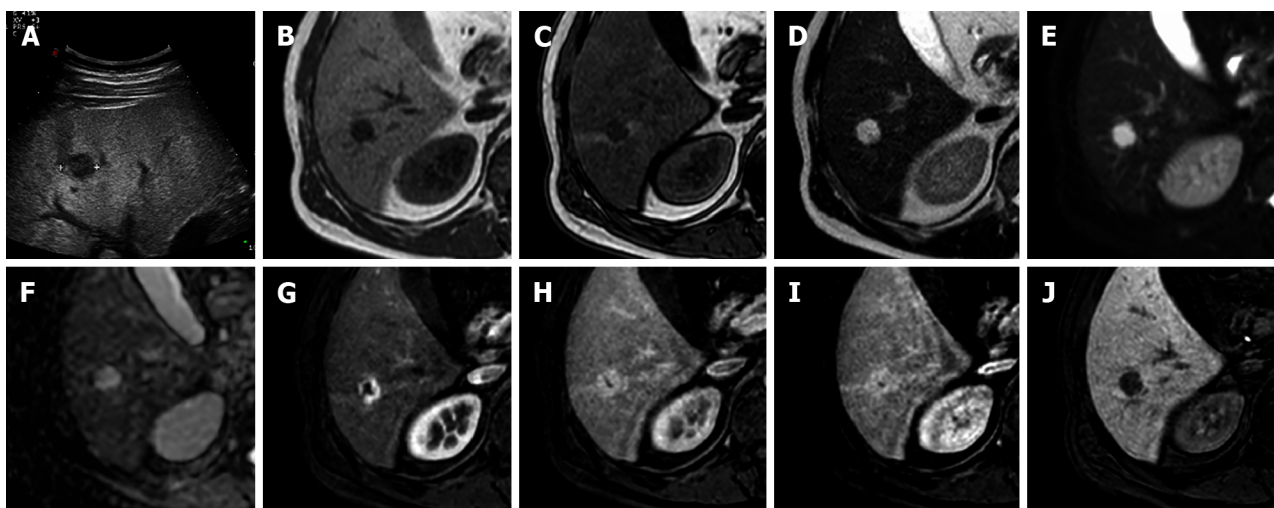


**Figure 9 A 42-year-old male underwent ultrasound examination for abdominal discomfort demonstrating diffuse steatosis with a hypoechoic nodule in S6.** Liver magnetic resonance imaging confirmed diffuse steatosis and a hypointense lesion on T1-weighted sequences, hyperintense on long TR sequences and on the ADC map. During dynamic study after intravenous contrast injection, the lesion presents centripetal enhancement and is hypointense on the hepatobiliary phase. These features are consistent with hemangioma. A: Liver ultrasound image; B: In-phase T1-weighted image; C: Out-of-phase T1-weighted image; D: T2-weighted image; E: T2-Spectral Attenuated Inversion Recovery; F: ADC map; G: Arterial phase magnetic resonance imaging (MRI); H: Portal venous phase MRI; I: Delayed phase MRI; J: Hepatobiliary phase MRI.

sequences, indicating intralesional fat components[46] (Figure 11).

Lesions with minimal fat content (angiomatous or myomatous types) are more difficult to characterize and are frequently classified as HCC because of their appearance on morphologic sequences and after contrast injection: They show moderate to high signal intensity on T2-weighted sequences, hypointensity on T1-weighted sequences, and early dishomogeneous contrast enhancement during contrast-enhanced dynamic studies with CEUS, CT, and MRI, with longer duration[47].

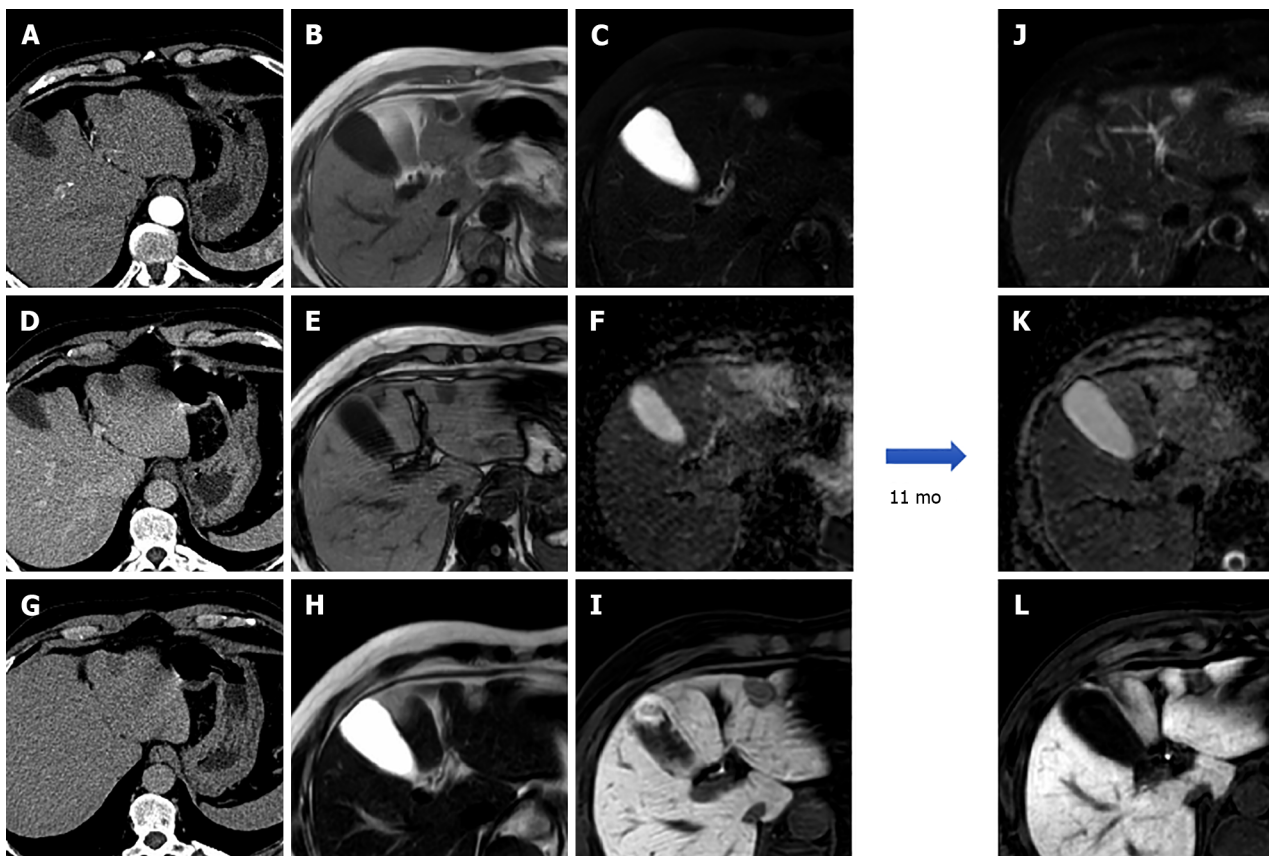


**Figure 10** A 57-year-old male underwent abdominal computed tomography scan with contrast for the evaluation of a renal mass demonstrating a hepatic lesion in S3, hypodense on contrast-enhanced computed tomography. Liver magnetic resonance imaging (MRI) confirmed the presence of a nodule hypointense on T1-weighted sequences, slightly hyperintense on long TR sequences, without significant restriction on the ADC map. During dynamic study after intravenous contrast injection (gadoxetic acid), the lesion does not have significant enhancement and it appears hypointense on the hepatobiliary phase. At 11 mo follow-up, the nodule shows stable dimensions and MRI signal features. These features are consistent with fibrous hemangioma. A: Arterial phase of liver computed tomography (CT); B: In-phase T1-weighted image; C: T2-Spectral Attenuated Inversion Recovery; D: Portal venous phase of liver CT; E: Out-of-phase T1-weighted image; F: ADC map; G: Delayed phase of liver CT; H: T2-weighted image; I: Hepatobiliary phase (HBP) magnetic resonance imaging (MRI); J: T2-Spectral Attenuated Inversion Recovery; K: ADC map; L: HBP MRI.

Recent studies have established the utility of DWI-MRI with ADC values in the differential diagnosis of HAMls and HCCs with fat components as HAMls have higher values than HCCs with fat. Since HAML does not contain hepatocytes, it appears hypointense in the HBP[47].

### Lymphangioma

Hepatic lymphangioma (HL), a malformation of the lymphatic system is a rare benign liver neoplasm. Most lymphangiomas are located outside the abdominal cavity, being less than 5% intra-abdominal, affecting primarily the small bowel mesentery, followed by the omentum, mesocolon, and retroperitoneum. Liver location is usually seen when lymphangiomas affect multiple organs, as in lymphangiomatosis. Solitary HL is rarely seen and could lead to clinical misdiagnosis[48,49].

HLs are histologically classified into capillary lymphangioma, cystic lymphangioma, and cavernous lymphangioma. They may occur at any age, with an average age of 30 years and a slightly higher incidence in females[48,50]. HL may be asymptomatic and incidentally found on cross-sectional imaging. The symptoms, if present, usually depend on compression of adjacent organs by the neoplasm [51].

Imaging appearances of HLs are various. On US they may be non-echoic, low-echoic, and mixed-echoic masses containing cystic and solid components within unicystic chamber or multichambers. On CT scanning a unilocular cystic mass shows low density and no enhancement. In some cases, it may present like a low-density mass with enhancement. For a multilocular mass with mixed components, enhancement is observed in the septum and solid parts but not in the cystic components. However, some cases described in the literature show atypical appearance, for example with wash-in and wash-out in the solid component mimicking malignancy[48,51].

MRI of HL shows a low signal on T1-weighted imaging, high signal on T2-weighted imaging, and occasionally mixed signals, related to intralesional bleeding that may occur. In the case of microcystic lymphangioma mistaken for a solid mass depending on its enhancement after intravenous injection of contrast, MRI with T2-weighted imaging may be very useful in the detection of multiple microcysts. The

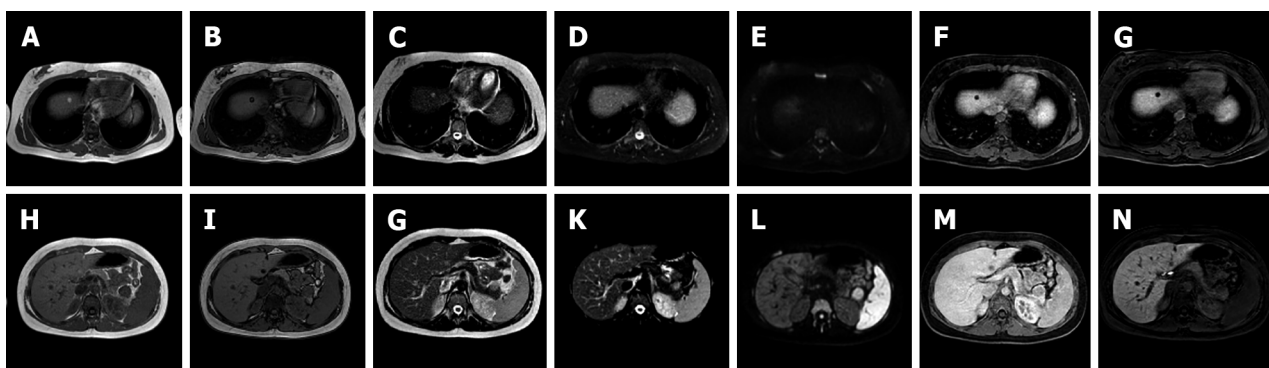


**Figure 11 A 20-year-old female with tuberous sclerosis.** Liver magnetic resonance imaging demonstrates a small focal lesion in S8 hyperintense on in-phase T1-weighted images, with signal loss on opposed-phase sequences with marginal india-ink artifact because of chemical shift, hyperintense on T2 turbo spin echo sequences, hypointense on T2-Spectral Attenuated Inversion Recovery (SPAIR) images, without increased signal on diffusion weighted images and hypointense in all phases during dynamic study and on the hepatobiliary phase (HBP). These features are consistent with lipoma. A second nodule in S2-S3 depicts a hyperintense signal on in-phase T1-weighted images, with signal loss on opposed-phase sequence, hyperintense on T2-TSE images, hypointense on T2-SPAIR sequences, without increased signal on diffusion weighted images. The nodule presents minimal vascularization during dynamic study and appears hypointense on HBP, such features are compatible with angiomyolipoma. A: In-phase T1-weighted image; B: Out-of-phase T1-weighted image; C: T2-weighted image; D: T2-Spectral Attenuated Inversion Recovery (SPAIR); E: High *b*-value diffusion weighted imaging; F: Portal venous phase magnetic resonance imaging (MRI); G: Hepatobiliary phase (HBP) MRI; H: In-phase T1-weighted image; I: Out-of-phase T1-weighted image; J: T2-weighted image; K: T2-SPAIR; L: High *b*-value diffusion weighted imaging; M: portal venous phase MRI; N: HBP MRI.

presentation of enhancement is similar to that of enhanced CT[48,52].

Diagnosis of lymphangioma is difficult due to a lack of typical symptoms and signs and differential diagnosis from simple cyst, BCA, BCAC, hydatid cyst, sclerosing HA, or HCC is very difficult[52]. Definitive diagnosis relied on pathological examination, that can be necessary in a cirrhotic liver with a lesion diameter less than 2 cm and if the cystic appearance is not predominant on imaging[48].

Macroscopically, the cysts resemble unilocular cysts or multilocular cysts of varying diameters with a septum, some of which have solid material or are filled with clear serous fluid, chylous fluid, and blood clots. Solid components have the microscopic appearance of fibrous hyperplasia, whilst liquid components are made up of a high number of cystic-dilated lymphatic lumens lined by simple squamous endothelium and filled with lymph. If morphology is insufficient to make a diagnosis, lymphatic markers and D2-40 (podoplanin) may be used to confirm the condition. Furthermore, endothelial markers such as von Willebrand factor, CD31, CD34, and two lymphatic markers (LYVE-1 and Prox-1) are utilized to identify lymphatic vessels from blood vessels immunohistochemically[53].

### Solitary fibrous tumor

Solitary fibrous tumor (SFT) is a rare soft tissue neoplasm that originates from mesenchymal tissue. It was first reported in 1931 as an intra-thoracic mass arising from the pleura. Even if cases of SFT have been reported to originate in organs external to the thorax, hepatic location is extremely rare, accounting for less than 100 cases in the literature[54,55].

Liver SFT appears as a large, well-defined and heterogeneous single lesion that usually involves the right hepatic lobe, with a median tumor size of 17 cm[54,56]. It may occur at any age, with a prevalence in middle-aged women[56]. SFT is asymptomatic in 80% of patients. Symptoms depend on tumor effects, including pain, weight loss and nausea, and less frequently weakness, fever and hypoglycemia. Laboratory parameters are usually non-specific[57]. SFT does not reveal specific findings on imaging examination.

Ultrasonography often shows a heterogeneous mass that may be low-echoic, hyperechoic or both, with or without calcifications. On CT scan it shows early arterial enhancement with delayed venous wash-out. MRI may reveal a heterogeneous lesion, slightly hyperintense on T2-weighted sequences and hypointense on T1-weighted sequences, with a high signal on DWI[55]. In some cases reported in the literature, the imaging appearance of SFT with gadoxetic acid shows heterogeneous enhancement on arterial and portal phase images and homogeneous hypointensity on HBP[54,58].

As these findings are non-specific and mimic those of HCC or leiomyomas, the diagnosis of SFT is challenging, as these tumors have no typical symptoms and signs[55]. A definitive diagnosis relied on histopathological and immunohistochemical studies[55]. On histology, SFT is characterized by fibroblast-like spindle cells within thick collagen bundles, with patternless architecture in which hypo and hypercellular areas coexist; collagenous stroma contains hemangiopericytic vessels. Immunohistochemical reactions are usually positive for CD34 in most of cases, but the specific immunohistochemical marker of SFT is STAT6[55,59].

The biological behavior of SFT is controversial, in fact it may show malignant potential, as described in some reported cases of metastasis or recurrence[54,57,59]. England *et al*[60] in 1989 reported

malignancy criteria: the presence of intratumoral necrosis or hemorrhage, mitotic changes, pleomorphism of cellular nuclei, metastasis, large dimensions (more than 10 cm) and cellular atypia[59].

### **Mesenchymal hamartoma**

Mesenchymal hamartoma (MH) of the liver is a rare benign tumor that originates from an anomalous development of primitive portal mesenchymal tissue, comprising predominantly of a mesenchymal stromal component and an aberrant malformed biliary structure with a small amount of hepatic lobules [61].

This neoplasm usually affects children mainly in the first 2 years with a slightly male predominance and it accounts for 8% of liver tumors in children[61-63]. Liver MH appears as a large benign multicystic/solid cystic liver mass, sometimes pedunculated, arising in the right lobe of the liver in 75% of cases[64].

MH has non-specific clinical manifestations, usually depending on the size of the tumor, which can reach up to 30 cm. Patients may present with hepatomegaly, a non-tender abdominal mass causing occlusion of the inferior vena cava or dyspnea and sometimes with fever, weight loss or vomiting. Alpha-fetoprotein is usually normal[61]. Imaging appearance depends on the cystic, solid/cystic or solid predominance of the tumor[61,64].

US often shows a complex cystic mass with internal septation[65]. On CT scan it shows a heterogeneous appearance with enhancing stromal elements and cystic components with water attenuation [64]. The stromal component may be predominant in some cases, although cystic components are more frequent and may vary in size; if the lesion is predominantly cystic it may range from a "swiss cheese appearance" if cysts are small, into a multilocular cystic lesion with septa, if the cystic components are large[61,64]. MRI appearance depends on the cystic vs stromal composition of the neoplasm and on the protein content of the fluid. The solid component may be hypointense to adjacent liver both on T1-weighted and T2-weighted sequences due to fibrosis. Cystic components usually show signal intensity similar to water on T2-weighted images and may have variable signal intensity on T1-weighted sequences owing to the protein content of cystic areas. After injection of gadolinium only stromal components and septa were enhanced[64].

On histology, a fibromyxoid connective background with bland spindle cells characterizes MH with branching bile ducts, thick walled vascular channels and scattered island of hepatocytes in the periphery of the lesion[66]. The biological behavior of MH is benign, although cases of malignant degeneration in undifferentiated embryonal sarcoma are described in the literature[65].

---

## **PSEUDOTUMOR**

---

### **Focal fatty infiltration**

Focal fatty hepatic infiltration can be easily recognized using the standard liver MRI examination, based on T1-weighted in-phase/out-of-phase and T2-weighted images, which in the latter shows a slight hypointense signal. However, in some cases, these focal areas can be misdiagnosed as focal liver lesions and they have to be assessed using dynamic contrast enhancement and HBP imaging. Considering the physiological GD-BOPTA and Gd-EOB-DTPA uptake by normal hepatocytes, the focal fatty infiltration or hypersteatosis areas have decreased contrast enhancement due to a reduced number of functioning hepatocytes or atypical vascularization. Moreover, in the case of nodular-shaped focal fatty infiltration, its differential diagnosis with a fat-containing liver lesion can be challenging. In this setting, a wedge or pyramidal shape and the lack of mass effect are useful features to distinguish a focal fatty lesion from a focal liver lesion[67] (Figure 12).

Yeom et al[68], by evaluating 27 focal fat deposition areas, reported a homogeneous or heterogeneous enhancement during the dynamic study, both in the arterial and portal venous phase, with hypointense signal during HBP. On the other hand, fat spared areas do not show any signal drop-off during in-phase/out-of-phase imaging and may induce increased signal intensity on HBP due to preserved or increased focal liver function[69].

### **Infection-liver abscess**

The liver abscess, defined as a localized collection of inflammatory products caused by bacterial, fungal or parasitic agents, can be easily diagnosed with all imaging techniques, but is best with US and CT. MRI can help to distinguish between uni- and multi-focal necrotic lesions disseminated through the liver parenchyma. In this setting, the typical appearance of liver abscess during the standard MRI protocol can support the final diagnosis, based on the iso- to hyperintense appearance on T1-weighted images due to the presence of proteins, hemorrhagic foci, or inflammatory degradation products, without a significant drop-off in signal during in-phase/out-of-phase imaging. T2-weighted imaging is useful for determining not only the amount of free water inside the lesion but also to identify the slight peripheral hyperintense area due to edema or peripheral inflammation. Usually, on DWI an abscess presents a high restricted diffusion with very low values of ADC because of the high viscosity of inflammatory debris and cellularity[21] in the necrotic cavity, while no diffusion restriction is seen

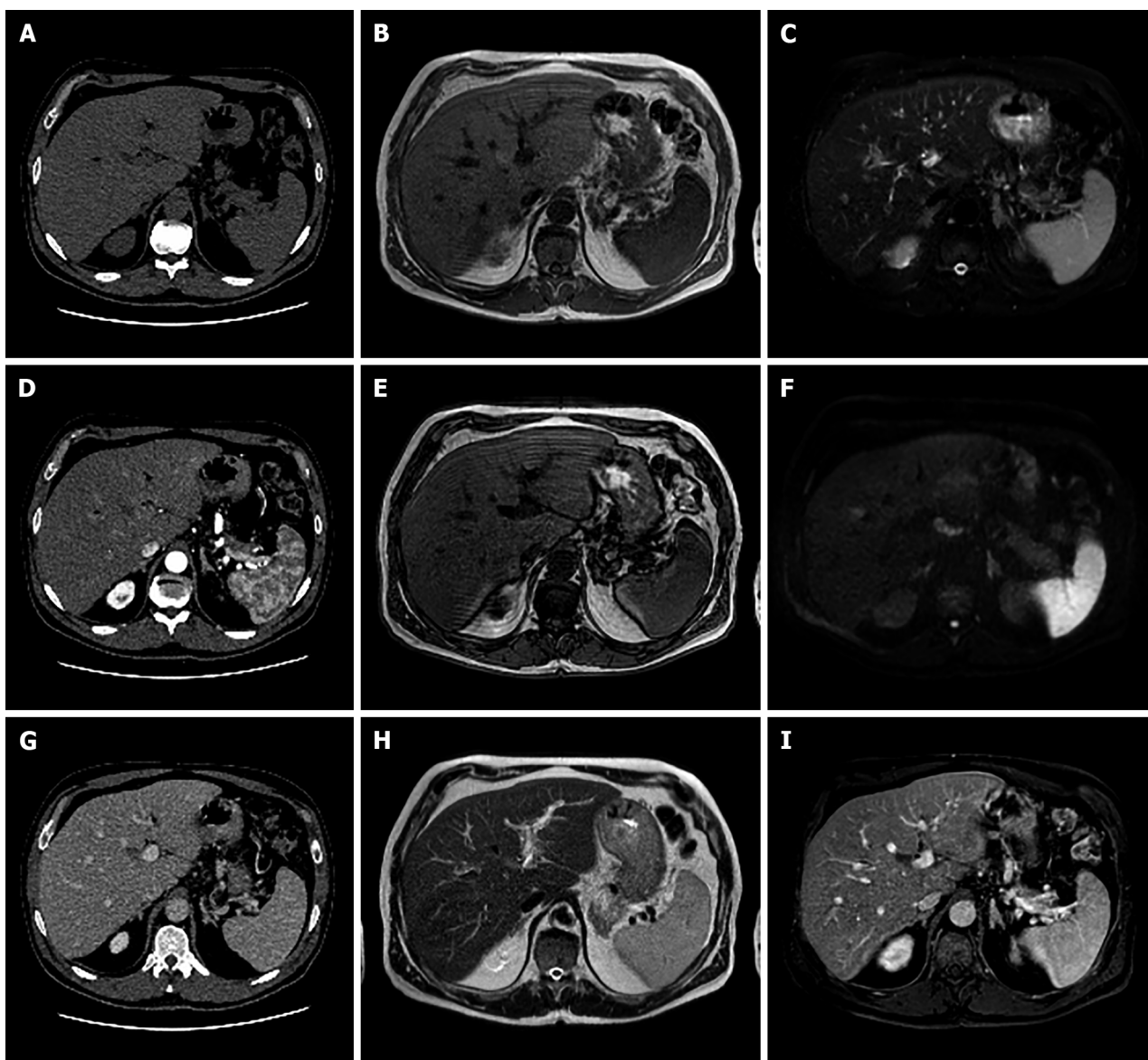


**Figure 12 A 50-year-old male, unremarkable past medical history.** Multiphase abdominal computed tomography study shows a hypodense liver area near the porta hepatis. Subsequent magnetic resonance imaging liver study confirmed a hilar area slightly hyperintense on T1 in-phase sequence, with signal loss on opposed-phase images, slightly hyperintense on T2-turbo spin echo images, hypointense on T2-Spectral Attenuated Inversion Recovery images, without significant increased signal on diffusion weighted images and with no contrast enhancement on dynamic study. These features are consistent with an area of focal fatty infiltration. A: Unenhanced liver computed tomography (CT); B: In-phase T1-weighted image; C: T2-Spectral Attenuated Inversion Recovery; D: Arterial phase of liver CT; E: Out-of-phase T1-weighted image; F: High *b*-value diffusion weighted imaging; G: Portal venous phase of liver CT; H: T2-weighted image; I: Portal venous phase magnetic resonance imaging.

peripherally. Furthermore, as reported by Park *et al*[70], DWI is helpful in differentiating hepatic abscess from malignant mimickers considering the higher peripheral restriction in the case of malignancy with 98% diagnostic accuracy.

During the dynamic study, liver abscess typically shows a peripheral rim enhancement, in particular on the portal-venous and delayed or transitional phase, due to the presence of a pseudocapsule and inflammatory cells. During the HBP, the core typically does not change in appearance, while the peripheral area can show an ipo- to isointense signal, due to edema or the normal function of hepatocytes, respectively (Figure 13).

Although size, shape, number, and signal intensity can help to establish a differential diagnosis, the only pathognomonic signs are the presence of air bubbles within the lesion or an air-fluid level[71], seen as a single or multiple flow-void foci. The most important differential diagnosis of liver abscess is metastasis. As mentioned above, liver metastasis can be recognized due to the different signal intensity on T2-weighted images and DWI with a slight and clear hyperintense appearance, respectively, as well as during the dynamic study, in particular with a poor peripheral ring enhancement due to the presence of pathological cells. On the portal-venous and transitional phase, solid liver metastases present an isointense signal while abscess shows a hypointense signal.

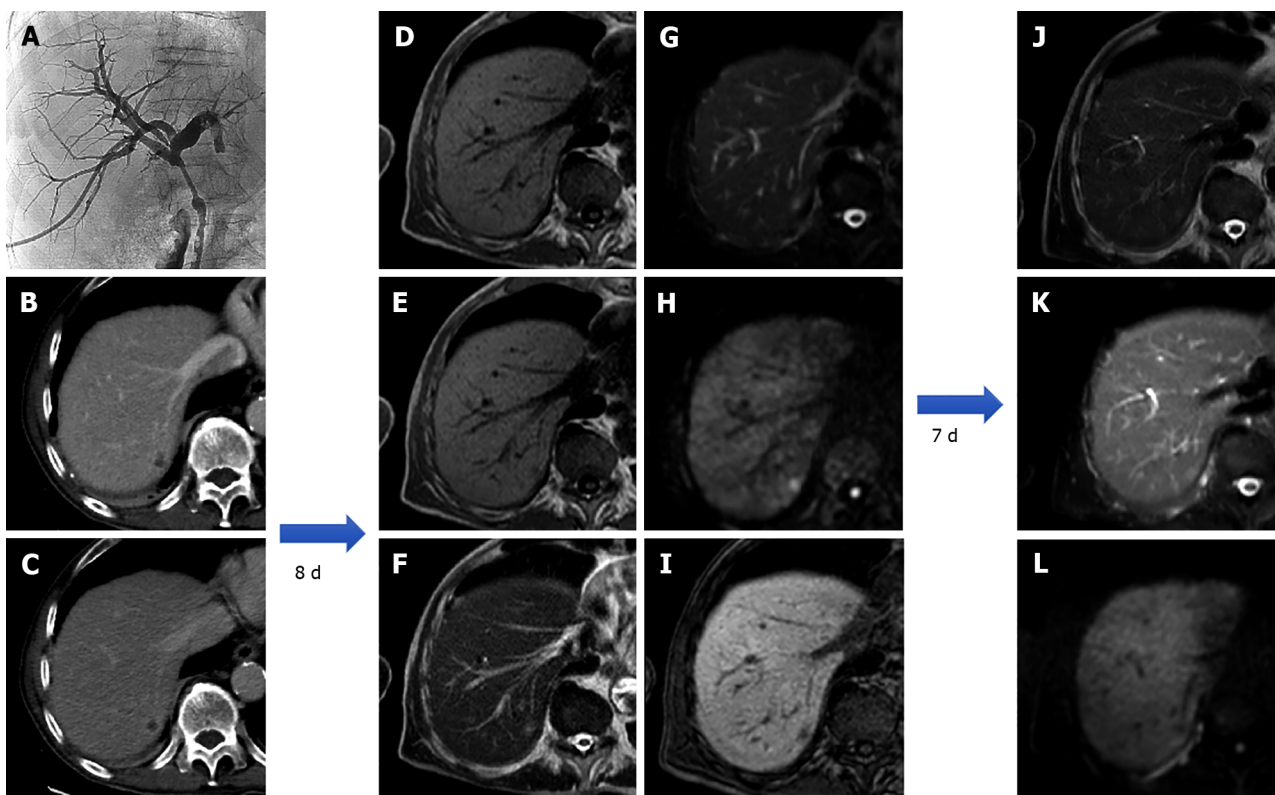


**Figure 13 An 80-year-old patient with the finding of common hepatic bile duct stenosis.** Cholangiography procedure with the placement of biliary drainage in which histological diagnosis of the biliary tract suggested adenocarcinoma of the main biliary duct. Following an episode of fever, increase in white blood cells ( $13.02 \times 10^9/L$ ) and C-reactive protein (90.1 mg/L) computed tomography examination showed a small hepatic hypodensity in the 7<sup>th</sup> segment. Liver magnetic resonance imaging (MRI) performed after a few days of therapy shows a nodular lesion, hypointense on the T1-weighted sequences, slightly hyperintense in the T2 sequences, with increased signal on diffusion weighted imaging (DWI) and hypointense signal on the hepatobiliary phase. A 7-d follow-up liver MRI examination showed a further evolution of the lesion with evidence of a very slight hyperintense signal on T2 sequences and almost disappearance of the lesion itself on DWI, which confirmed the diagnosis of hepatic abscess. A: Percutaneous transhepatic cholangiography; B: Portal venous phase of liver computed tomography (CT); C: Delayed phase of liver CT; D: In-phase T1-weighted image; E: Out-of-phase T1-weighted image; F: T2-weighted image; G: T2-Spectral Attenuated Inversion Recovery (SPAIR); H: High *b*-value diffusion weighted imaging; I: Hepatobiliary phase magnetic resonance imaging; L: T2-weighted image; M: T2-SPAIR; N: high *b*-value DWI.

To date, only one study has evaluated the importance of Gd-EOB-DTPA in distinguishing between hepatic microabscesses and metastasis: Choi *et al*[72], by enrolling 72 patients, demonstrated that perilesional edema and arterial rim enhancement were maintained during the following dynamic sequences. Also the size discrepancy between T1-weighted and T2-weighted images and between T1-weighted and HBP images, allow a high diagnostic accuracy for microabscess (90.9%).

#### Infection-Echinococcus granulosus

Different tapeworms belonging to the *Echinococcus* genus can infect humans, both as the intermediate or definitive host. The two most important types of disease are cystic echinococcosis and alveolar echinococcosis, caused by *Echinococcus granulosus* (*E. granulosus*) and *E. multilocularis*, respectively.

This subsection will focus on *E. granulosus* considering its higher incidence and global distribution in all countries except Antarctica[73]. Sheep and pigs are definitive hosts of *E. granulosus* and typically excrete hundreds of eggs within their feces. Intermediate hosts, such as dogs, cats, or humans, can eat these eggs directly or indirectly *via* contaminated water, food, or soil[74]. The tapeworm, following the blood vessels typically stops in the liver more frequently in the right lobe, where it starts growing as a cystic lesion, with a growth rate ranging from 1-2 mm to 10 mm per year. Cysts are composed of two layers of membrane: A germinal and an outer layer. The immune system responds to the cyst by forming a capsule that during years will be completely calcified[74].

When performing MRI, it should be taken into account that cystic echinococcosis can show different imaging features according to the parasitic stage in the infected liver. In the first stage of infection, a rounded, thin-walled cyst is recognizable, showing an inhomogeneous signal in T1-weighted images, hyperintense in T2-weighted images, with only peripheral enhancement best seen on the portal-venous or delayed phases. During cystic growth, it is possible to observe the typical echinococcosis cyst features, appreciable in approximately 75% of cases: The daughter cysts within the main cyst may produce a honeycomb-like structure with a typical thin peripheral capsule, hypointense both in T1-weighted and T2-weighted images. When the daughter cysts grow, the pressure inside the whole cyst

can lead to their collapse or rupture into the biliary tree or peritoneal seeding: Under this circumstance, the internal appearance may vary according to the amount of cystic debris, especially on T2-weighted images (Figure 14). Finally, the dead cyst is composed of a solid matrix, due to the immune response manifesting with the peripheral calcified layer, from partial to complete, that can be seen in about 50% of cases[75].

#### **Inflammatory disorder of the liver-pseudotumor**

Hepatic inflammatory pseudotumor, even if rare, has an unknown etiology and can manifest itself as a consequence of different immune responses, such as infective agents, including viruses (such as Epstein-Barr virus), bacteria and fungi (nocardia and actinomycosis), primary and secondary liver tumors including hepatic lymphoma[76], and as the hepatic manifestation of immunologic disease, such as IgG4-related disease[77], inflammatory bowel disease[78], and, finally, a response to a foreign body[79].

Hepatic pseudotumor can present as single or multiple lesions with a wide range of distribution, including liver parenchyma, peri-portal spaces, and peri-biliary ducts. On unenhanced MRI it can show a hypointensity signal on T1-weighted images, without any signal drop-off during in-phase/out-of-phase imaging, with variable signal intensity on T2-weighted images strictly linked to the presence of acute edema or, if chronic, fibrosis can be present. In line with the T2 signal, the pseudotumor can show areas of signal restriction on DWI, typically peripheral, due to the high cellularity of inflammatory cells.

Considering the mixed content within the lesion, during dynamic sequences the enhancement can be different. It can mimic a CCC with peripheral enhancement during the arterial phase with a delayed central-filling, in the case of diffuse fibrotic components; heterogeneous enhancement can be easily identified in the case of acute or subacute findings, while chronic lesion variable enhancement can be present. Sometimes it can also show internal septa with delayed enhancement. On HBP imaging, pseudotumor typically manifests as a hypointense lesion due to the small number of functioning hepatocytes, surrounded by fibro-inflammatory components. The abovementioned features were confirmed by a recent study published by Ichikawa *et al*[80], in which the typical appearance of pseudotumor was demonstrated, a central hypointense signal with a relatively peripheral hyperintensity on HBP, helping the differential diagnosis with colorectal liver metastasis.

#### **Inflammatory disorder of the liver-sarcoidosis**

Even if typically considered a thoracic disease, sarcoidosis can involve all human organs, with an estimated 50% of patients with extra-thoracic manifestations[81]. Based on the underlying pathophysiology, it can manifest as hepatomegaly with possible jaundice and with manifestations of portal hypertension, even if not commonly reported. Thus, liver MRI should be performed to exclude the presence of focal liver lesions. In patients with sarcoidosis the typical changes due to liver fibrosis were the most common findings, underlining that only 25% of patients showed normal liver morphology with no radiological signs of portal hypertension. In this setting, focal hepatic and splenic nodules were seen in about 25% of subjects at presentation, demonstrating coalescing granulomas sometimes confluent and mimicking malignancy[82]. The sarcoidosis nodules are usually hypointense on T1-weighted images, without any changes on in-phase/out-of-phase imaging, while a variable signal on T2-weighted images can be seen, ranging from hypo to hyperintensity, strictly linked to the amount of edema both intra- and peri-lesional. During enhanced sequences, these lesions may show a slight and peripheral enhancement on the arterial phase while during the next sequences, including the HPB, the lesions show hypointense signals (Figure 15). Sometimes the sarcoidosis can manifest exclusively with chronic liver failure.

---

## **CONCLUSION**

---

Liver lesions are common findings in radiologists' daily routine. They are a complex category of pathology that ranges from solitary benign lesions to primary liver cancer and liver metastases. Liver MRI is a fundamental radiological method in these patients as it allows with its multiparametric approach an optimal non-invasive tissue characterization. Liver MRI can be used to differentiate between pseudotumors and tumors, as well as benign and malignant lesions, and it can also be utilized for differential diagnosis. Although histological examination can be useful in making a definitive diagnosis, liver MRI is an important modality in the diagnosis of liver lesions with a significant impact on patient care.

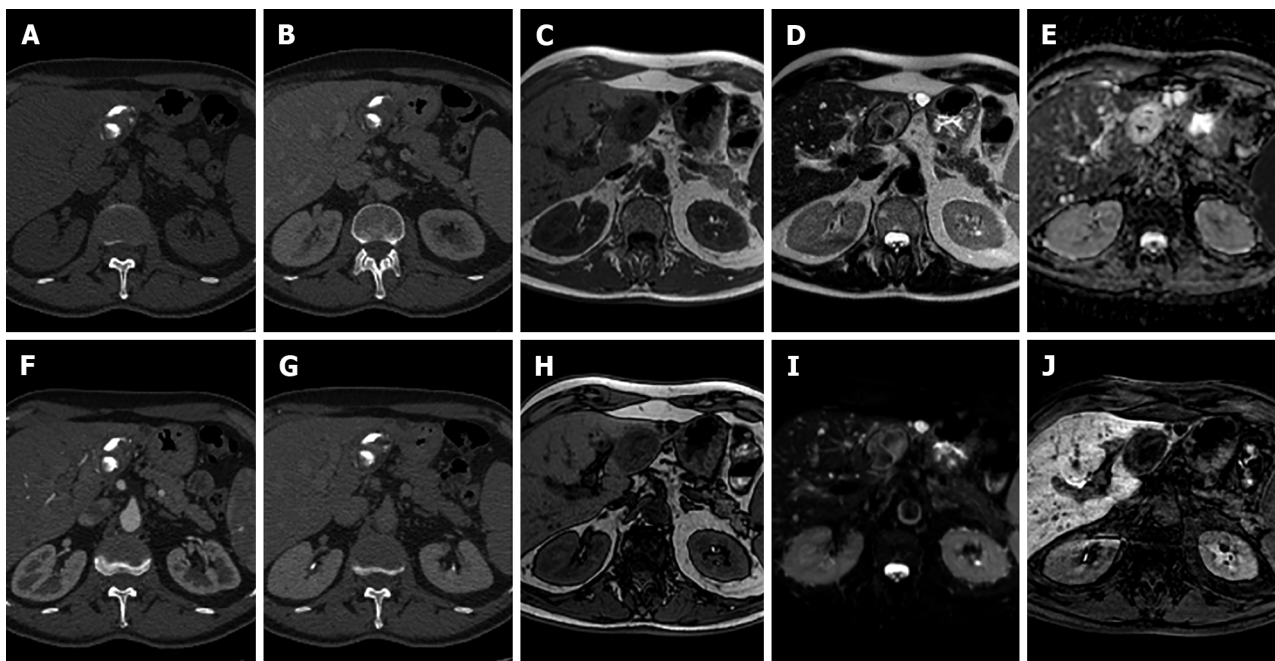


**Figure 14** A 67-year-old male who underwent multiphasic abdominal computed tomography scan demonstrated a lesion with gross calcifications in S3 that did not present contrast enhancement in any phase. Liver magnetic resonance imaging confirmed a nodular formation, hypointense on T1-weighted sequences, isointense on long TR sequences with more hypointense components corresponding to calcification on computed tomography images, without significant restriction on diffusion weighted images and hypointense on the hepatobiliary phase. These features are consistent with a calcified echinococcal cyst. A: Unenhanced liver computed tomography (CT); B: Portal venous phase of liver CT; C: In-phase T1-weighted image; D: T2-weighted image; E: ADC map; F: Portal venous phase of liver CT; G: Delayed phase of liver CT; H: Out-of-phase T1-weighted image; I: T2-Spectral Attenuated Inversion Recovery; L: Hepatobiliary phase magnetic resonance imaging.

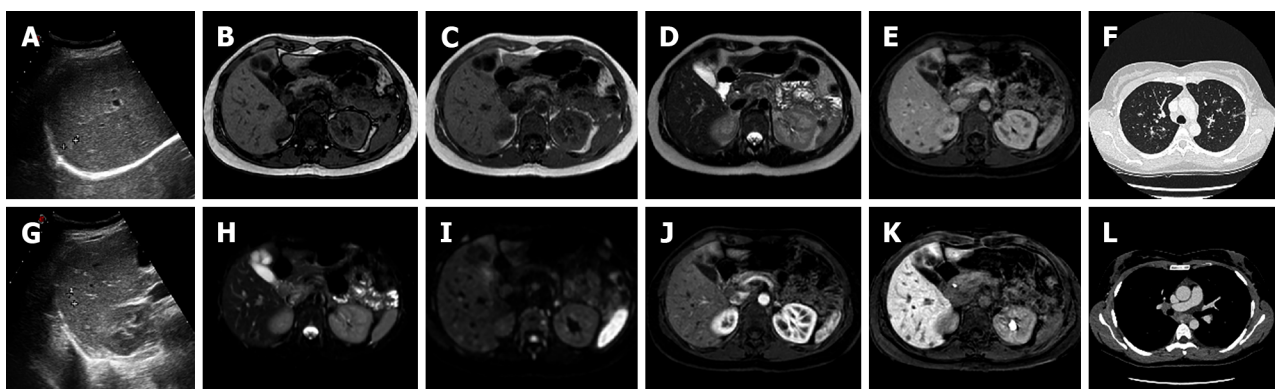


**Figure 15** A 38-year-old female, smoker, polycystic ovary syndrome, previous appendicectomy. Abdominal ultrasound performed due to neutropenia demonstrated hyperechoic liver nodules. Subsequent liver magnetic resonance imaging confirmed multiple liver nodules hypointense in T1-weighted sequences slightly hyperintense on T2 sequences, with increased signal on diffusion weighted images, without contrast enhancement after dynamic study with gadoxetic acid. Lesions are hypointense on the hepatobiliary phase. Chest computed tomography with contrast demonstrated bilateral nodules with a perilymphatic pattern and a bigger lesion with satellite nodules (galaxy sign) on the right; increased hilar lymph nodes were present. Transbronchial biopsy demonstrated noncaseating granulomas which led to the diagnosis of sarcoidosis. A: Liver ultrasound image; B: Out-of-phase T1-weighted image; C: In-phase T1-weighted image; D: T2-turbo spin echo; E: Portal venous phase magnetic resonance imaging (MRI); F: Chest computed tomography (CT) with pulmonary parenchymal window; G: Ultrasound image; H: T2-Spectral Attenuated Inversion Recovery; I: High b-value diffusion weighted imaging; J: Arterial phase MRI; K: Hepatobiliary phase MRI; L: Chest CT with mediastinal window.

## FOOTNOTES

**Author contributions:** Gatti M was involved in conception and design of the study; Gatti M, Maino C, Tore D, Carisio A and Tricarico E were involved in literature review, analysis and writing of the original draft; Darvizeh F was involved in writing of the original draft; Inchegnolo R and Ippolito D took part in supervision of the study; Faletti R took part in supervision of the study and is the guarantor of the study; and all the authors worked together to edit, review and approve the article.

**Conflict-of-interest statement:** The authors declare that there is no conflict of interest.

**Open-Access:** This article is an open-access article that was selected by an in-house editor and fully peer-reviewed by external reviewers. It is distributed in accordance with the Creative Commons Attribution NonCommercial (CC BY-NC 4.0) license, which permits others to distribute, remix, adapt, build upon this work non-commercially, and license their derivative works on different terms, provided the original work is properly cited and the use is non-commercial. See: <https://creativecommons.org/Licenses/by-nc/4.0/>

**Country/Territory of origin:** Italy

**ORCID number:** Marco Gatti 0000-0001-8168-5280; Cesare Maino 0000-0002-5742-802X; Davide Tore 0000-0002-5087-5740; Andrea Carisio 0000-0003-3957-7934; Fatemeh Darvizeh 0000-0002-3735-0472; Eleonora Tricarico 0000-0001-9805-2551; Riccardo Inchincarlo 0000-0002-0253-5936; Davide Ippolito 0000-0002-2696-7047; Riccardo Faletti 0000-0002-8865-8637.

**S-Editor:** Wang JJ

**L-Editor:** Webster JR

**P-Editor:** Cai YX

## REFERENCES

- 1 Li J, Wang J, Lei L, Yuan G, He S. The diagnostic performance of gadoxetic acid disodium-enhanced magnetic resonance imaging and contrast-enhanced multi-detector computed tomography in detecting hepatocellular carcinoma: a meta-analysis of eight prospective studies. *Eur Radiol* 2019; **29**: 6519-6528 [PMID: 31250172 DOI: 10.1007/s00330-019-06294-6]
- 2 Wang J, Ye X, Li J, He S. The diagnostic performance of gadoxetic acid disodium-enhanced magnetic resonance imaging and contrast-enhanced ultrasound in detecting hepatocellular carcinoma: A meta-analysis. *Medicine (Baltimore)* 2021; **100**: e24602 [PMID: 33578564 DOI: 10.1097/MD.00000000000024602]
- 3 Ippolito D, Inchincarlo R, Grazioli L, Drago SG, Nardella M, Gatti M, Faletti R. Recent advances in non-invasive magnetic resonance imaging assessment of hepatocellular carcinoma. *World J Gastroenterol* 2018; **24**: 2413-2426 [PMID: 29930464 DOI: 10.3748/wjg.v24.i23.2413]
- 4 Inchincarlo R, Faletti R, Grazioli L, Tricarico E, Gatti M, Pecorelli A, Ippolito D. MR with Gd-EOB-DTPA in assessment of liver nodules in cirrhotic patients. *World J Hepatol* 2018; **10**: 462-473 [PMID: 30079132 DOI: 10.4254/wjh.v10.i7.462]
- 5 Oldhafer KJ, Habbel V, Horling K, Makridis G, Wagner KC. Benign Liver Tumors. *Visc Med* 2020; **36**: 292-303 [PMID: 33005655 DOI: 10.1159/000509145]
- 6 Tsili AC, Alexiou G, Naka C, Argyropoulou MI. Imaging of colorectal cancer liver metastases using contrast-enhanced US, multidetector CT, MRI, and FDG PET/CT: a meta-analysis. *Acta Radiol* 2021; **62**: 302-312 [PMID: 32506935 DOI: 10.1177/0284185120925481]
- 7 Sporea I, Săndulescu DL, Şirli R, Popescu A, Danilă M, Spârchez Z, Mihai C, Ioanițescu S, Moga T, Timar B, Brisc C, Nedelcu D, Săftoiu A, Enăchescu V, Badea R. Contrast-Enhanced Ultrasound for the Characterization of Malignant versus Benign Focal Liver Lesions in a Prospective Multicenter Experience - The SRUMB Study. *J Gastrointestin Liver Dis* 2019; **28**: 191-196 [PMID: 31204417 DOI: 10.15403/jgld-180]
- 8 Inchincarlo R, Maino C, Gatti M, Tricarico E, Nardella M, Grazioli L, Sironi S, Ippolito D, Faletti R. Gadoxetic acid magnetic-enhanced resonance imaging in the diagnosis of cholangiocarcinoma. *World J Gastroenterol* 2020; **26**: 4261-4271 [PMID: 32848332 DOI: 10.3748/wjg.v26.i29.4261]
- 9 Grazioli L, Faletti R, Frittoli B, Battisti G, Ambrosini R, Romanini L, Gatti M, Fonio P. Evaluation of incidence of acute transient dyspnea and related artifacts after administration of gadoxetate disodium: a prospective observational study. *Radiol Med* 2018; **123**: 910-917 [PMID: 30084108 DOI: 10.1007/s11547-018-0927-y]
- 10 Zhang L, Yu X, Huo L, Lu L, Pan X, Jia N, Fan X, Morana G, Grazioli L, Schneider G. Detection of liver metastases on gadobenate dimeglumine-enhanced MRI: systematic review, meta-analysis, and similarities with gadoxetate-enhanced MRI. *Eur Radiol* 2019; **29**: 5205-5216 [PMID: 30915560 DOI: 10.1007/s00330-019-06110-1]
- 11 Castaldo A, De Lucia DR, Pontillo G, Gatti M, Cocozza S, Ugga L, Cuocolo R. State of the Art in Artificial Intelligence and Radiomics in Hepatocellular Carcinoma. *Diagnostics (Basel)* 2021; **11** [PMID: 34209197 DOI: 10.3390/diagnostics11071194]
- 12 Laumonier H, Bioulac-Sage P, Laurent C, Zucman-Rossi J, Balabaud C, Trillaud H. Hepatocellular adenomas: magnetic resonance imaging features as a function of molecular pathological classification. *Hepatology* 2008; **48**: 808-818 [PMID: 18688875 DOI: 10.1002/hep.22417]
- 13 Shanbhogue AK, Prasad SR, Takahashi N, Vikram R, Sahani DV. Recent advances in cytogenetics and molecular biology of adult hepatocellular tumors: implications for imaging and management. *Radiology* 2011; **258**: 673-693 [PMID: 21339346 DOI: 10.1148/radiol.10100376]
- 14 Dharmana H, Sarvana-Bawan S, Girgis S, Low G. Hepatocellular adenoma: imaging review of the various molecular subtypes. *Clin Radiol* 2017; **72**: 276-285 [PMID: 28126185 DOI: 10.1016/j.crad.2016.12.020]
- 15 Lin H, van den Esschert J, Liu C, van Gulik TM. Systematic review of hepatocellular adenoma in China and other regions. *J Gastroenterol Hepatol* 2011; **26**: 28-35 [PMID: 21175790 DOI: 10.1111/j.1440-1746.2010.06502.x]
- 16 Baum JK, Bookstein JJ, Holtz F, Klein EW. Possible association between benign hepatomas and oral contraceptives. *Lancet* 1973; **2**: 926-929 [PMID: 4126557 DOI: 10.1016/s0140-6736(73)92594-4]
- 17 Edmondson HA, Reynolds TB, Henderson B, Benton B. Regression of liver cell adenomas associated with oral contraceptives. *Ann Intern Med* 1977; **86**: 180-182 [PMID: 835939 DOI: 10.7326/0003-4819-86-2-180]

- 18 **Flejou JF**, Barge J, Menu Y, Degott C, Bismuth H, Potet F, Benhamou JP. Liver adenomatosis. An entity distinct from liver adenoma? *Gastroenterology* 1985; **89**: 1132-1138 [PMID: 2412930]
- 19 **Donato M**, Hamidian Jahromi A, Andrade AI, Kim R, Chaudhery SI, Sangster G. Hepatic adenomatosis: a rare but important liver disease with severe clinical implications. *Int Surg* 2015; **100**: 903-907 [PMID: 26011213 DOI: 10.9738/INTSURG-D-14-00161.1]
- 20 **Ronot M**, Bahrami S, Calderaro J, Valla DC, Bedossa P, Belghiti J, Vilgrain V, Paradis V. Hepatocellular adenomas: accuracy of magnetic resonance imaging and liver biopsy in subtype classification. *Hepatology* 2011; **53**: 1182-1191 [PMID: 21480324 DOI: 10.1002/hep.24147]
- 21 **Grazioli L**, Ambrosini R, Frittoli B, Grazioli M, Morone M. Primary benign liver lesions. *Eur J Radiol* 2017; **95**: 378-398 [PMID: 28987695 DOI: 10.1016/j.ejrad.2017.08.028]
- 22 **Bioulac-Sage P**, Laumonier H, Couchy G, Le Bail B, Sa Cunha A, Rullier A, Laurent C, Blanc JF, Cubel G, Trillaud H, Zucman-Rossi J, Balabaud C, Saric J. Hepatocellular adenoma management and phenotypic classification: the Bordeaux experience. *Hepatology* 2009; **50**: 481-489 [PMID: 19585623 DOI: 10.1002/hep.22995]
- 23 **Dhingra S**, Fiel MI. Update on the new classification of hepatic adenomas: clinical, molecular, and pathologic characteristics. *Arch Pathol Lab Med* 2014; **138**: 1090-1097 [PMID: 25076298 DOI: 10.5858/arpa.2013-0183-RA]
- 24 **Nguyen BN**, Fléjou JF, Terris B, Belghiti J, Degott C. Focal nodular hyperplasia of the liver: a comprehensive pathologic study of 305 lesions and recognition of new histologic forms. *Am J Surg Pathol* 1999; **23**: 1441-1454 [PMID: 10584697 DOI: 10.1097/00000478-199912000-00001]
- 25 **Cogley JR**, Miller FH. MR imaging of benign focal liver lesions. *Radiol Clin North Am* 2014; **52**: 657-682 [PMID: 24889166 DOI: 10.1016/j.rcl.2014.02.005]
- 26 **Gatti M**, Calandri M, Bergamasco L, Darvizeh F, Grazioli L, Inchegolo R, Ippolito D, Rousset S, Veltre A, Fonio P, Faletti R. Characterization of the arterial enhancement pattern of focal liver lesions by multiple arterial phase magnetic resonance imaging: comparison between hepatocellular carcinoma and focal nodular hyperplasia. *Radiol Med* 2020; **125**: 348-355 [PMID: 31916102 DOI: 10.1007/s11547-019-01127-4]
- 27 **Hussain SM**, Terkivatan T, Zondervan PE, Lanjouw E, de Rave S, Ijzermans JN, de Man RA. Focal nodular hyperplasia: findings at state-of-the-art MR imaging, US, CT, and pathologic analysis. *Radiographics* 2004; **24**: 3-17; discussion 18 [PMID: 14730031 DOI: 10.1148/rg.241035050]
- 28 **Ferlicot S**, Kobeiter H, Tran Van Nhieu J, Cherqui D, Dhumeaux D, Mathieu D, Zafrani ES. MRI of atypical focal nodular hyperplasia of the liver: radiology-pathology correlation. *AJR Am J Roentgenol* 2004; **182**: 1227-1231 [PMID: 15100124 DOI: 10.2214/ajr.182.5.1821227]
- 29 **Jahic E**, Sofic A, Selimovic AH. DWI/ADC in Differentiation of Benign from Malignant Focal Liver Lesion. *Acta Inform Med* 2016; **24**: 244-247 [PMID: 27708485 DOI: 10.5455/aim.2016.24.244-247]
- 30 **Agnello F**, Ronot M, Valla DC, Sinkus R, Van Beers BE, Vilgrain V. High-b-value diffusion-weighted MR imaging of benign hepatocellular lesions: quantitative and qualitative analysis. *Radiology* 2012; **262**: 511-519 [PMID: 22143926 DOI: 10.1148/radiol.11110922]
- 31 **Mortelé KJ**, Praet M, Van Vlierberghe H, Kunnen M, Ros PR. CT and MR imaging findings in focal nodular hyperplasia of the liver: radiologic-pathologic correlation. *AJR Am J Roentgenol* 2000; **175**: 687-692 [PMID: 10954451 DOI: 10.2214/ajr.175.3.1750687]
- 32 **Goodwin MD**, Dobson JE, Sirlin CB, Lim BG, Stella DL. Diagnostic challenges and pitfalls in MR imaging with hepatocyte-specific contrast agents. *Radiographics* 2011; **31**: 1547-1568 [PMID: 21997981 DOI: 10.1148/rg.316115528]
- 33 **Del Poggio P**, Buonocore M. Cystic tumors of the liver: a practical approach. *World J Gastroenterol* 2008; **14**: 3616-3620 [PMID: 18595127 DOI: 10.3748/wjg.14.3616]
- 34 **Guo Y**, Jain D, Weinreb J. Von Meyenburg Complex: Current Concepts and Imaging Misconceptions. *J Comput Assist Tomogr* 2019; **43**: 846-851 [PMID: 31356525 DOI: 10.1097/RCT.0000000000000904]
- 35 **Torbenson MS**. Hamartomas and malformations of the liver. *Semin Diagn Pathol* 2019; **36**: 39-47 [PMID: 30579648 DOI: 10.1053/j.semdp.2018.11.005]
- 36 **Zheng RQ**, Zhang B, Kudo M, Onda H, Inoue T. Imaging findings of biliary hamartomas. *World J Gastroenterol* 2005; **11**: 6354-6359 [PMID: 16419165 DOI: 10.3748/wjg.v11.i40.6354]
- 37 **Semelka RC**, Hussain SM, Marcos HB, Woosley JT. Biliary hamartomas: solitary and multiple lesions shown on current MR techniques including gadolinium enhancement. *J Magn Reson Imaging* 1999; **10**: 196-201 [PMID: 10441025 DOI: 10.1002/(sici)1522-2586(199908)10:2<196::aid-jmri14>3.0.co;2-r]
- 38 **Giambelluca D**, Caruana G, Cannella R, Lo Re G, Midiri M. The starry sky liver: multiple biliary hamartomas on MR cholangiopancreatography. *Abdom Radiol (NY)* 2018; **43**: 2529-2530 [PMID: 29411059 DOI: 10.1007/s00261-018-1490-7]
- 39 **Evans J**, Willyard CE, Sabih DE. Cavernous Hepatic Hemangiomas. 2021 Nov 5. In: StatPearls [Internet]. Treasure Island (FL): StatPearls Publishing; 2022 Jan-. [PMID: 29262074]
- 40 **Chan YL**, Lee SF, Yu SC, Lai P, Ching AS. Hepatic malignant tumour versus cavernous haemangioma: differentiation on multiple breath-hold turbo spin-echo MRI sequences with different T2-weighting and T2-relaxation time measurements on a single slice multi-echo sequence. *Clin Radiol* 2002; **57**: 250-257 [PMID: 12014868 DOI: 10.1053/crad.2001.0763]
- 41 **Parikh T**, Drew SJ, Lee VS, Wong S, Hecht EM, Babb JS, Taouli B. Focal liver lesion detection and characterization with diffusion-weighted MR imaging: comparison with standard breath-hold T2-weighted imaging. *Radiology* 2008; **246**: 812-822 [PMID: 18223123 DOI: 10.1148/radiol.2463070432]
- 42 **Vilgrain V**, Boulos L, Vullierme MP, Denys A, Terris B, Menu Y. Imaging of atypical hemangiomas of the liver with pathologic correlation. *Radiographics* 2000; **20**: 379-397 [PMID: 10715338 DOI: 10.1148/radiographics.20.2.g00mc01379]
- 43 **Klotz T**, Montoriol PF, Da Ines D, Petitcolin V, Joubert-Zakeyh J, Garcier JM. Hepatic haemangioma: common and uncommon imaging features. *Diagn Interv Imaging* 2013; **94**: 849-859 [PMID: 23796395 DOI: 10.1016/j.diii.2013.04.008]
- 44 **Ridge CA**, Shia J, Gerst SR, Do RK. Sclerosed hemangioma of the liver: concordance of MRI features with histologic characteristics. *J Magn Reson Imaging* 2014; **39**: 812-818 [PMID: 24783239 DOI: 10.1002/jmri.24228]
- 45 **Boraschi P**, Donati F, Gherarducci G. Imaging findings in myomatous angiomyolipoma of the liver. *Diagn Interv Radiol*

- 2012; **18**: 387-390 [PMID: 22517073 DOI: 10.4261/1305-3825.DIR.4870-11.2]
- 46 **Zhu Z**, Yang L, Zhao XM, Luo DQ, Zhang HT, Zhou CW. Myomatous hepatic angiomyolipoma: imaging findings in 14 cases with radiological-pathological correlation and review of the literature. *Br J Radiol* 2014; **87**: 20130712 [PMID: 24670055 DOI: 10.1259/bjr.20130712]
- 47 **Wang SY**, Kuai XP, Meng XX, Jia NY, Dong H. Comparison of MRI features for the differentiation of hepatic angiomyolipoma from fat-containing hepatocellular carcinoma. *Abdom Imaging* 2014; **39**: 323-333 [PMID: 24389893 DOI: 10.1007/s00261-013-0070-0]
- 48 **Long X**, Zhang L, Cheng Q, Chen Q, Chen XP. Solitary hepatic lymphangioma mimicking liver malignancy: A case report and literature review. *World J Clin Cases* 2020; **8**: 4633-4643 [PMID: 33083428 DOI: 10.12998/wjcc.v8.i19.4633]
- 49 **Losanoff JE**, Richman BW, El-Sherif A, Rider KD, Jones JW. Mesenteric cystic lymphangioma. *J Am Coll Surg* 2003; **196**: 598-603 [PMID: 12691938 DOI: 10.1016/S1072-7515(02)01755-6]
- 50 **Alqahtani A**, Nguyen LT, Flageole H, Shaw K, Laberge JM. 25 years' experience with lymphangiomas in children. *J Pediatr Surg* 1999; **34**: 1164-1168 [PMID: 10442614 DOI: 10.1016/s0022-3468(99)90590-0]
- 51 **Huang L**, Li J, Zhou F, Yan J, Liu C, Zhou AY, Tang A, Yan Y. Giant cystic lymphangioma of the liver. *Hepatol Int* 2010; **4**: 784-787 [PMID: 21286352 DOI: 10.1007/s12072-010-9220-4]
- 52 **Choi WJ**, Jeong WK, Kim Y, Kim J, Pyo JY, Oh YH. MR imaging of hepatic lymphangioma. *Korean J Hepatol* 2012; **18**: 101-104 [PMID: 22511911 DOI: 10.3350/kjhep.2012.18.1.101]
- 53 **Matsumoto T**, Ojima H, Akishima-Fukasawa Y, Hiraoka N, Onaya H, Shimada K, Mizuguchi Y, Sakurai S, Ishii T, Kosuge T, Kanai Y. Solitary hepatic lymphangioma: report of a case. *Surg Today* 2010; **40**: 883-889 [PMID: 20740355 DOI: 10.1007/s00595-010-4255-7]
- 54 **Makino Y**, Miyazaki M, Shigekawa M, Ezaki H, Sakamori R, Yakushijin T, Ohkawa K, Kato M, Akasaka T, Shinzaki S, Nishida T, Miyake Y, Hama N, Nagano H, Honma K, Morii E, Wakasa K, Hikita H, Tatsumi T, Iijima H, Hiramatsu N, Tsujii M, Takehara T. Solitary fibrous tumor of the liver from development to resection. *Intern Med* 2015; **54**: 765-770 [PMID: 25832939 DOI: 10.2169/internalmedicine.54.3053]
- 55 **Yugawa K**, Yoshizumi T, Mano Y, Kurihara T, Yoshiya S, Takeishi K, Itoh S, Harada N, Ikegami T, Soejima Y, Kohashi K, Oda Y, Mori M. Solitary fibrous tumor in the liver: case report and literature review. *Surg Case Rep* 2019; **5**: 68 [PMID: 31020464 DOI: 10.1186/s40792-019-0625-6]
- 56 **Andaluz García I**, Tavecchia M, Olveira Martín A. A solitary fibrous tumor: an entity to consider in the diagnosis of liver masses. *Rev Esp Enferm Dig* 2019; **111**: 969 [PMID: 31696720 DOI: 10.17235/reed.2019.6433/2019]
- 57 **Shu Q**, Liu X, Yang X, Guo B, Huang T, Lei H, Peng F, Su S, Li B. Malignant solitary fibrous tumor of the liver: a case report. *Int J Clin Exp Pathol* 2019; **12**: 2305-2310 [PMID: 31934058]
- 58 **Nam HC**, Sung PS, Jung ES, Yoon SK. Solitary fibrous tumor of the liver mimicking malignancy. *Korean J Intern Med* 2020; **35**: 734-735 [PMID: 30836742 DOI: 10.3904/kjim.2018.442]
- 59 **Rouy M**, Guilbaud T, Birnbaum DJ. Liver Solitary Fibrous Tumor: a Rare Incidentaloma. *J Gastrointest Surg* 2021; **25**: 852-853 [PMID: 32607857 DOI: 10.1007/s11605-020-04701-8]
- 60 **England DM**, Hochholzer L, McCarthy MJ. Localized benign and malignant fibrous tumors of the pleura. A clinicopathologic review of 223 cases. *Am J Surg Pathol* 1989; **13**: 640-658 [PMID: 2665534 DOI: 10.1097/00000478-198908000-00003]
- 61 **Maqbool H**, Mushtaq S, Hassan U, Ahmad AH, Sarwar S, Sheikh UN. Case series of Mesenchymal Hamartoma: a Rare Childhood Hepatic Neoplasm. *J Gastrointest Cancer* 2020; **51**: 1030-1033 [PMID: 32124239 DOI: 10.1007/s12029-020-00374-3]
- 62 **Lack EE**. Mesenchymal hamartoma of the liver. A clinical and pathologic study of nine cases. *Am J Pediatr Hematol Oncol* 1986; **8**: 91-98 [PMID: 3740369]
- 63 **Kim SH**, Kim WS, Cheon JE, Yoon HK, Kang GH, Kim IO, Yeon KM. Radiological spectrum of hepatic mesenchymal hamartoma in children. *Korean J Radiol* 2007; **8**: 498-505 [PMID: 18071280 DOI: 10.3348/kjr.2007.8.6.498]
- 64 **Rosado E**, Cabral P, Campo M, Tavares A. Mesenchymal hamartoma of the liver--a case report and literature review. *J Radiol Case Rep* 2013; **7**: 35-43 [PMID: 23705055 DOI: 10.3941/jrcr.v7i5.1334]
- 65 **Martins-Filho SN**, Putra J. Hepatic mesenchymal hamartoma and undifferentiated embryonal sarcoma of the liver: a pathologic review. *Hepat Oncol* 2020; **7**: HEP19 [PMID: 32647564 DOI: 10.2217/hep-2020-0002]
- 66 **Siddiqui MA**, McKenna BJ. Hepatic mesenchymal hamartoma: a short review. *Arch Pathol Lab Med* 2006; **130**: 1567-1569 [PMID: 17090204 DOI: 10.5858/2006-130-1567-HMHASR]
- 67 **Venkatesh SK**, Yin M, Ehman RL. Magnetic resonance elastography of liver: technique, analysis, and clinical applications. *J Magn Reson Imaging* 2013; **37**: 544-555 [PMID: 23423795 DOI: 10.1002/jmri.23731]
- 68 **Yeom SK**, Byun JH, Kim HJ, Park SH, Kim N, Shin YM, Kim PN. Focal fat deposition at liver MRI with gadobenate dimeglumine and gadoxetic acid: Quantitative and qualitative analysis. *Magn Reson Imaging* 2013; **31**: 911-917 [PMID: 23598063 DOI: 10.1016/j.mri.2013.02.002]
- 69 **Ünal E**, İdilman İS, Karaosmanoğlu AD, Özmen MN, Akata D, Karcaaltincaba M. Hyperintensity at fat spared area in steatotic liver on the hepatobiliary phase MRI. *Diagn Interv Radiol* 2019; **25**: 416-420 [PMID: 31650968 DOI: 10.5152/dir.2019.18535]
- 70 **Park HJ**, Kim SH, Jang KM, Lee SJ, Park MJ, Choi D. Differentiating hepatic abscess from malignant mimickers: value of diffusion-weighted imaging with an emphasis on the periphery of the lesion. *J Magn Reson Imaging* 2013; **38**: 1333-1341 [PMID: 23559325 DOI: 10.1002/jmri.24112]
- 71 **Lardiére-Deguelte S**, Ragot E, Amroun K, Piardi T, Dokmak S, Bruno O, Appere F, Sibert A, Hoeffel C, Sommacale D, Kianmanesh R. Hepatic abscess: Diagnosis and management. *J Visc Surg* 2015; **152**: 231-243 [PMID: 25770745 DOI: 10.1016/j.jviscsurg.2015.01.013]
- 72 **Choi SY**, Kim YK, Min JH, Cha DI, Jeong WK, Lee WJ. The value of gadoxetic acid-enhanced MRI for differentiation between hepatic microabscesses and metastases in patients with periampullary cancer. *Eur Radiol* 2017; **27**: 4383-4393 [PMID: 28342102 DOI: 10.1007/s00330-017-4782-3]
- 73 **Deplazes P**, Rinaldi L, Alvarez Rojas CA, Torgerson PR, Harandi MF, Romig T, Antolova D, Schurer JM, Lahmar S,

- Cringoli G, Magambo J, Thompson RC, Jenkins EJ. Global Distribution of Alveolar and Cystic Echinococcosis. *Adv Parasitol* 2017; **95**: 315-493 [PMID: 28131365 DOI: 10.1016/bs.apar.2016.11.001]
- 74 **Pakala T**, Molina M, Wu GY. Hepatic Echinococcal Cysts: A Review. *J Clin Transl Hepatol* 2016; **4**: 39-46 [PMID: 27047771 DOI: 10.14218/JCTH.2015.00036]
- 75 **Doyle DJ**, Hanbridge AE, O'Malley ME. Imaging of hepatic infections. *Clin Radiol* 2006; **61**: 737-748 [PMID: 16905380 DOI: 10.1016/j.crad.2006.03.010]
- 76 **Kaneko R**, Mitomi H, Nakazaki N, Yano Y, Ogawa M, Sato Y. Primary Hepatic Lymphoma Complicated by a Hepatic Inflammatory Pseudotumor and Tumor-Forming Pancreatitis. *J Gastrointestin Liver Dis* 2017; **26**: 299-304 [PMID: 28922443 DOI: 10.15403/jgld.2014.1121.263.eko]
- 77 **Hamano A**, Yamada R, Kurata K, Tsuboi J, Inoue H, Tanaka K, Horiki N, Takei Y. Difficulty in differentiating between IgG4-related hepatic inflammatory pseudotumor and intrahepatic cholangiocarcinoma. *Clin J Gastroenterol* 2021; **14**: 263-268 [PMID: 33037585 DOI: 10.1007/s12328-020-01245-x]
- 78 **Schafer E**, Shyu I, Walker C, Smallfield G. New Presentation of Hepatic Inflammatory Pseudotumor and Crohn Disease. *Inflamm Bowel Dis* 2020; **26**: e97-e98 [PMID: 32561902 DOI: 10.1093/ibd/izaa138]
- 79 **Zhou J**, Zhan S, Zhu Q, Gong H, Wang Y, Fan D, Gong Z, Huang Y. Prediction of nodal involvement in primary rectal carcinoma without invasion to pelvic structures: accuracy of preoperative CT, MR, and DWIBS assessments relative to histopathologic findings. *PLoS One* 2014; **9**: e92779 [PMID: 24695111 DOI: 10.1371/journal.pone.0092779]
- 80 **Ichikawa S**, Motosugi U, Suzuki T, Shimizu T, Onishi H. Imaging features of hepatic inflammatory pseudotumor: distinction from colorectal liver metastasis using gadoxetate disodium-enhanced magnetic resonance imaging. *Abdom Radiol (NY)* 2020; **45**: 2400-2408 [PMID: 32468212 DOI: 10.1007/s00261-020-02575-7]
- 81 **Cremers J**, Drent M, Driessen A, Nieman F, Wijnen P, Baughman R, Koek G. Liver-test abnormalities in sarcoidosis. *Eur J Gastroenterol Hepatol* 2012; **24**: 17-24 [PMID: 22008629 DOI: 10.1097/MEG.0b013e32834c7b71]
- 82 **Jung G**, Brill N, Poll LW, Koch JA, Wettstein M. MRI of hepatic sarcoidosis: large confluent lesions mimicking malignancy. *AJR Am J Roentgenol* 2004; **183**: 171-173 [PMID: 15208133 DOI: 10.2214/ajr.183.1.1830171]



Published by **Baishideng Publishing Group Inc**  
7041 Koll Center Parkway, Suite 160, Pleasanton, CA 94566, USA

**Telephone:** +1-925-3991568

**E-mail:** [bpgoffice@wjnet.com](mailto:bpgoffice@wjnet.com)

**Help Desk:** <https://www.f6publishing.com/helpdesk>

<https://www.wjnet.com>

